

**ITERATIVE MAP AND APRI-SOVA
RECEIVERS FOR THE FREQUENCY SELECTIVE
RAYLEIGH FADING CHANNEL**

by

Jiahuai Zhou

A Thesis Presented to the Faculty of Graduate Studies
in Partial Fulfilment of the Requirements
for the degree of

MASTER OF SCIENCE

Department of Electrical and Computer Engineering
University of Manitoba
Winnipeg MAnitoba
R3T 2N2 Canada

(c) February 1998



**National Library
of Canada**

**Acquisitions and
Bibliographic Services**

**395 Wellington Street
Ottawa ON K1A 0N4
Canada**

**Bibliothèque nationale
du Canada**

**Acquisitions et
services bibliographiques**

**395, rue Wellington
Ottawa ON K1A 0N4
Canada**

Your file Votre référence

Our file Notre référence

The author has granted a non-exclusive licence allowing the National Library of Canada to reproduce, loan, distribute or sell copies of this thesis in microform, paper or electronic formats.

The author retains ownership of the copyright in this thesis. Neither the thesis nor substantial extracts from it may be printed or otherwise reproduced without the author's permission.

L'auteur a accordé une licence non exclusive permettant à la Bibliothèque nationale du Canada de reproduire, prêter, distribuer ou vendre des copies de cette thèse sous la forme de microfiche/film, de reproduction sur papier ou sur format électronique.

L'auteur conserve la propriété du droit d'auteur qui protège cette thèse. Ni la thèse ni des extraits substantiels de celle-ci ne doivent être imprimés ou autrement reproduits sans son autorisation.

0-612-32293-9

**THE UNIVERSITY OF MANITOBA
FACULTY OF GRADUATE STUDIES

COPYRIGHT PERMISSION PAGE**

**ITERATIVE MAP AND APRI-SOVA RECEIVERS FOR THE
FREQUENCY SELECTIVE RAYLEIGH FADING CHANNEL**

BY

JIAHUAI ZHOU

**A Thesis/Practicum submitted to the Faculty of Graduate Studies of The University
of Manitoba in partial fulfillment of the requirements of the degree
of
MASTER OF SCIENCE**

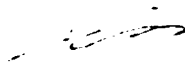
Jiahuai Zhou

©1998

Permission has been granted to the Library of The University of Manitoba to lend or sell copies of this thesis/practicum, to the National Library of Canada to microfilm this thesis and to lend or sell copies of the film, and to Dissertations Abstracts International to publish an abstract of this thesis/practicum.

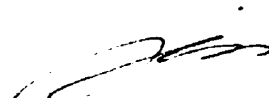
The author reserves other publication rights, and neither this thesis/practicum nor extensive extracts from it may be printed or otherwise reproduced without the author's written permission.

I hereby declare that I am the sole author of this thesis. I authorize the University of Manitoba to lend this thesis to other institutions or individuals for the purpose of scholarly research.



Jiahuai Zhou

I further authorize the University of Manitoba to reproduce this thesis by photocopying or by other means, in whole or in part, at the request of other institutions or individuals for the purpose of scholarly research.



Jiahuai Zhou

Acknowledgements

I would like to thank my advisor, Prof. Edward Shwedyk for his continuous support throughout this research effort. His technical guidance and encouragement during this endeavour helped me carry it to its successful completion. Moreover, I have benefited from his excellent teaching in four of my graduate courses. Grateful acknowledgement is due to the University of Manitoba for its financial support through graduate studies fellowship and Gordon P. Osler graduate scholarship. Special thanks also go to Weiyi Tang, for his helpful discussion and comments.

Finally, I acknowledge the understanding and support of my wife, Nanlan. She makes it all worthwhile.

Abstract

Two receivers, an iterative MAP receiver and an iterative Apri-SOVA receiver have been developed for joint demodulation and decoding of signals transmitted over the frequency selective Rayleigh fading channel. The proposed receivers are two stage suboptimal receivers and can detect coded signals with interleaving. Also because the soft-input, soft-output MAP and SOVA algorithms are used, there is no information lost between the stages. When the iterative processing technique is applied, the whole receiver's performance is close to optimal.

The error performance of the iterative receivers for the frequency selective Rayleigh fading channel have been studied with computer simulation. The results indicate that significant gain can be obtained with the first iteration. Compared to the MAP receiver, the Apri-SOVA receiver is simpler in its structure and computation, moreover a large size interleaver can be used with it without increasing the computation complexity. This makes the Apri-SOVA receiver more attractive in a practical application.

Contents

List of Figure

Abstract

1. Introduction	1
2. Background	7
2.1 General frequency selective Rayleigh fading channel model	7
2.2 ARMA channel model and Kalman filter	15
3. Symbol-by-symbol MAP joint demodulation and decoding	20
3.1 Symbol-by-symbol MAP demodulation	22
3.2 Joint demodulation and decoding with iterative MAP processing	28
3.3 Simulation Results	32
3.4 Summary	36

4. Joint Demodulation and Decoding with the Apri-SOVA	
Algorithm	41
4.1 Apri-SOVA demodulation	41
4.2 Iterative demodulation and decoding with Apri-SOVA	47
4.2.1 Convolutional codes	47
4.2.2 Metric for Apri-SOVA decoder	47
4.2.3 Soft-encoder	48
4.3 Simulation Results	49
5. Conclusions	57
5.1 Conclusions	57
5.2 Suggestions for further study	58
References	60

List of Figure

1-1	Block diagram of a digital communication system	4
1-2	Two stage receiver structure	5
2-1	Multipath Phenomena	8
2-2	A typical plane wave component incident on a vehicle receiver	9
2-3	$\phi_c(\tau)$, $v(\Delta t)$ and their Fourier transforms	12
2-4	A typical digital communication system for the frequency selective Rayleigh fading channel	14
2-5	Frequency selective Rayleigh fading channel model	15
2-6	Finite state space model for the Rayleigh fading channel	16
2-7	The MLSE-VA receiver for the frequency selective Rayleigh fading channel	19
3-1	Iterative receiver for frequency selective fading channels	21
3-2	Trellis for a fading channel with memory β and input $\{b\}$	23
3-3	MAP demodulator for frequency selective Rayleigh fading channels	29
3-4	Serially concatenated convolutional code and its iterative decoder	30
3-5	(a) Digital transmission system and (b) its equivalent serially concatenated encoder for convolutional encoder, interleaver and frequency selective fading channel	31
3-6	Iterative MAP demodulation and decoding algorithm for the frequency selective Rayleigh fading channel	32

3-7 Simulation block diagram	35
3-8 BER performance of MAP demodulation for the frequency selective Rayleigh fading channel	37
3-9 BER performance of MAP demodulation and decoding for the frequency selective Rayleigh fading channel	38
3-10 BER performance of iterative MAP receiver for a slow fading channel	39
3-11 BER performance of iterative MAP receiver for a fast fading channel	40
4-1 Apri-SOVA demodulator and an iterative Apri-SOVA receiver	43
4-2 The metric for Apri-SOVA demodulation	46
4-3 (2,1,6) Soft Encoder	50
4-4 Simulation Block Diagram for the Apri-SOVA Receiver	51
4-5 BER performance of Apri-SOVA demodulation for the frequency selective Rayleigh fading channel	53
4-6 BER performance of Apri-SOVA demodulation and decoding for the frequency selective Rayleigh fading channel	54
4-7 BER performance of iterative Apri-SOVA receiver for the slow fading channel	55
4-8 BER performance of iterative Apri-SOVA receiver for the fast fading channel	56

Chapter 1

Introduction

A mobile radio signal is most susceptible to the effects of multipath fading phenomena, which is caused by reflection, scattering and diffraction. Usually as the mobile unit moves through space, the received signals will be affected by attenuation and intersymbol interference (ISI) which makes communication over the wireless mobile channel very challenging.

A lot of research has been done in this field. In the early days of study, the signal distortion caused by multipath fading was the main concern, and techniques like coding and diversity were proposed to improve the reliability of communication [1-4]. With the increasing demand for high speed communication, random intersymbol interference caused by limited channel bandwidth and/or severe multipath spread becomes the most important factor to influence the performance of the communication system. One of the first techniques developed to reduce ISI was equalization [6]. Recently, maximum likelihood sequence estimation (MLSE) has been used [9]. Adaptive decision feedback equalization (DFE), due to its simplicity and flexibility, is most attractive and considerable research on it has been done [5-7]. However, one problem with DFE is that a long training sequence will not help to track the channel changes when the channel is a fast fading channel [8]. Also since with the DFE, it is difficult to produce soft decisions, soft decision decod-

ing is very difficult to realize. In comparison to DFE, MLSE though more complex, offers a significant performance improvement.

Using MLSE to reduce or remove ISI was first proposed by Forney [9]. The receiver consists of a linear filter (whitened matched filter), a symbol rate sampler and a Viterbi Algorithm (VA) processor. As shown in [9], the ISI can be expressed easily using a trellis structure. Based on the entire observation, the Viterbi algorithm is used to search the most likely transmitted sequence through the trellis.

When the channel is time-varying, MLSE requires an estimate of the channel impulse response (CIR). For a slowly varying channel, several kinds of adaptive MLSE receiver have been proposed [10-12]. When the channel is fast fading, the adaptive MLSE receivers mentioned above can not track the changes in the channel. Therefore channel estimation techniques are proposed to be used with MLSE.

Pilot-aided channel estimation was applied to the frequency nonselective Rayleigh fading channel by D'Andrea, Diglio and Mengali [13]. Kong [14] studied the frequency nonselective Rayleigh fading channel with MLSE-PD (preliminary decision - PD). Use of a Kalman filter to track the channel variation was proposed by Lodge and Moher [15]. For the special case of a frequency nonselective Rayleigh fading channel, they showed that a bank of linear FIR filters can be used to replace the Kalman filters. Thus the receiver has a simple structure. Dai and Shwedyk [16] extended their idea to the frequency selective Rayleigh fading channel and used a vector autoregressive moving average (ARMA) model to describe the channel. A bank of Kalman filters were

used to estimate the channel impulse response and calculate the branch metrics for the VA. In order to simplify the receiver structure, a suboptimal sequential algorithm was also proposed. Innovations-based MLSE for Rayleigh fading channel was proposed by Yu and Pasupathy[17], where, instead of using Kalman filters, a bank of FIR prediction filters were used. This yielded the same results as Kalman filters. Work on reducing the computational complexity has been done by Rollins and Simmons [18], where a parametric algorithm and a breadth-first reduced-search trellis decoding algorithm were applied to simplify the receiver. The results show that an order $O(N^2)$ reduction in complexity can be obtained with a modest increase in receiver error rate performance.

Today's digital communication systems are becoming more and more complex. Fig. 1.1 shows a general block diagram of a typical digital communication system. The encoder, interleaver, modulator and even the fading channel shown in Fig.1.1 usually contain memory. Therefore when one tries to perform optimal demodulation and decoding in one stage, all these memory units increase the number of states in the trellis (which grows exponentially with the memory length of the received signals), and make the receiver very complex, indeed impractical. One possible solution is to decompose the problem, i.e. to perform the demodulation and decoding several stages (as shown in Fig.1.1). The output from each stage could be in the form of "hard" decisions or "soft" decisions. Since soft-decision decoding achieves more coding gain than hard-decision decoding, only the stages with soft-input and soft-output are considered in this thesis.

When demodulation and decoding are performed in several stages, one question is: is the performance of this kind receiver optimal? If not, then another question is: how to obtain optimal or near-optimal performance in this case? As an example, Fig. 2 shows a two-stage receiver

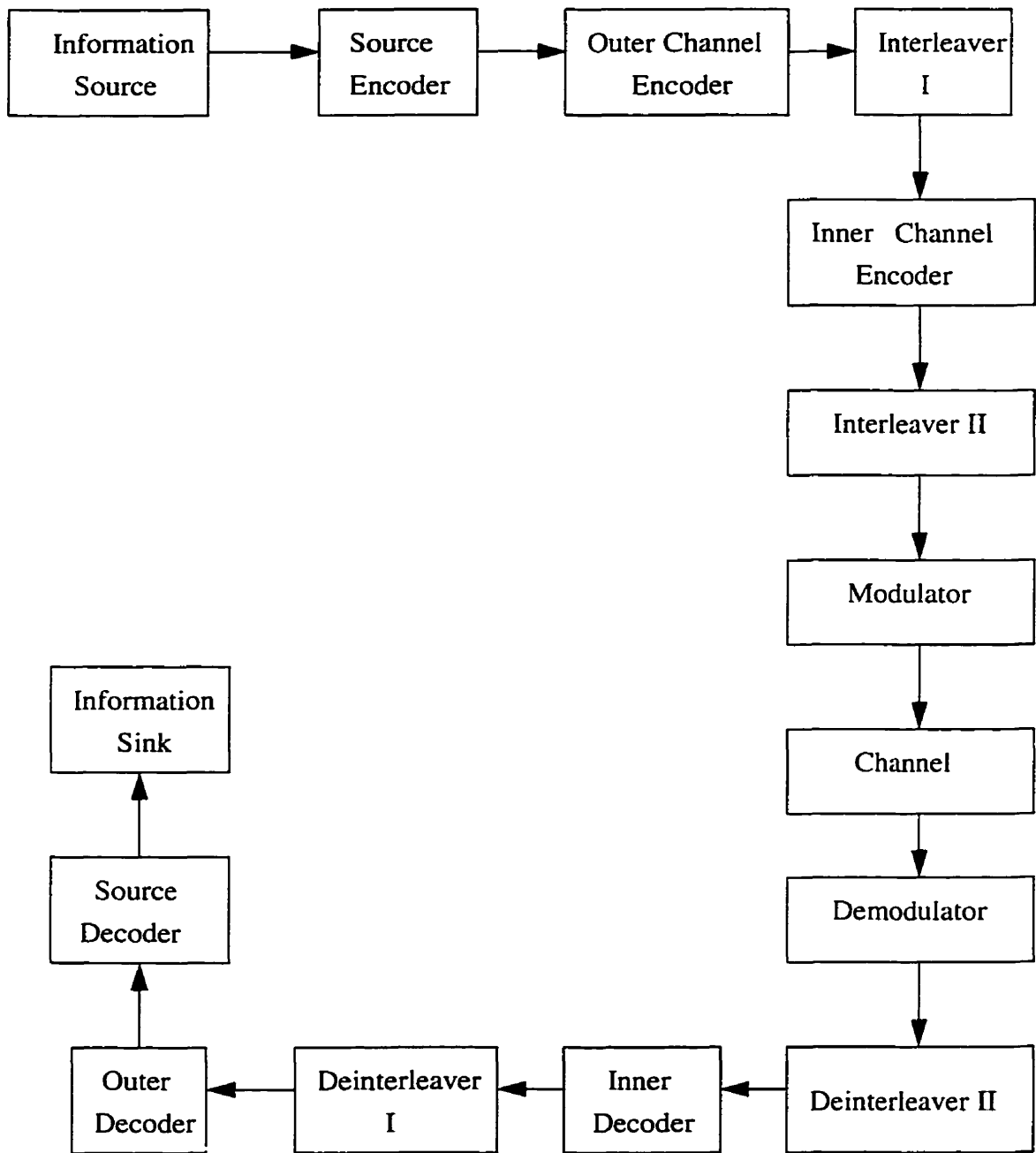


Figure 1.1 Block diagram of a digital communication system

structure. Studying the demodulation and decoding process tells that the decoding stage can use the soft information output from the demodulation stage, but the demodulation can not use the information supplied by the coding structure, thus the overall performance can be far from optimal. A very natural idea to solve this problem is to feedback to the demodulation stage soft information output from the decoding stage, which leads to an iterative processing approach. Recent work has shown that substantial coding gains can be obtained by iterative MAP processing techniques. Turbo coding is one of most successful and dramatic examples [19-20] of this. In [21], Gertsman and Lodge applied iterative MAP processing techniques to joint demodulation and decoding of CPM signals over Rayleigh flat-fading channels. The simulation results show that “the bit error performance of the iterative MAP receiver can approach that of a receiver operating with perfect knowledge of the fading process” [21].

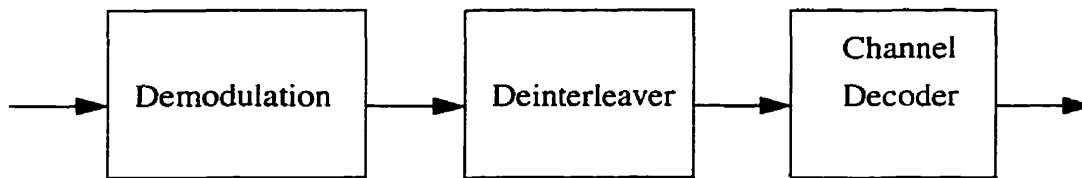


Figure 1.2 Two stage receiver structure

To the best of the author’s knowledge, there is no published research on the application of the soft iterative processing techniques for joint demodulation and decoding of signals transmitted over the frequency selective Rayleigh fading channel. This is the objective of this thesis.

The organization of this thesis is as follow. In chapter 2, background material is summarized, a general Rayleigh fading channel model and its vector ARMA representation are discussed. Also briefly presented in chapter 2 is the principle of using the Kalman filter as a channel estimator.

Chapter 3 applies the soft iterative processing technique to the frequency selective Rayleigh fading channel, where the symbol-by-symbol MAP algorithm is used. The required algorithm is derived and the error performance of the proposed iterative MAP receiver is studied by computer simulation.

To simplify the receiver structure, instead of the MAP algorithm, a low complexity algorithm, the soft-input, soft-output Viterbi algorithm (Apri-SOVA), is developed and studied in chapter 4. The metric used by Apri-SOVA demodulator in the frequency selective fading channel is derived and the computer simulation is done.

Finally, conclusions and suggestions for further research are given in chapter 5.

Chapter 2

Background

As background material for the rest of the thesis, a general Rayleigh fading channel model, its vector ARMA representation and the principle of using the Kalman filter as a channel estimator are presented in this chapter. The material follows closely references [22] and [23].

2.1 General frequency selective Rayleigh fading channel model

When a radio signal is transmitted between a fixed base station and a vehicle, it will be reflected and scattered by the surrounding terrain (see Fig. 2.1), which results in a multipath fading channel. The signal transmitted via different paths suffers different attenuation and propagation delay and the received signal is the weighted sum of them.

Let $s(t)$ be the transmitted signal, it can be written as

$$s(t) = \text{Re} [u(t) \cdot \exp(j2\pi f_c t)] \quad (2.1)$$

where $u(t)$ is the equivalent complex baseband signal and f_c is the carrier frequency. The received signal $x(t)$, coming from N signal paths, can be expressed as

$$x(t) = \sum_{n=1}^N \alpha_n(t) \cdot s(t - \tau_n(t)) \quad (2.2)$$

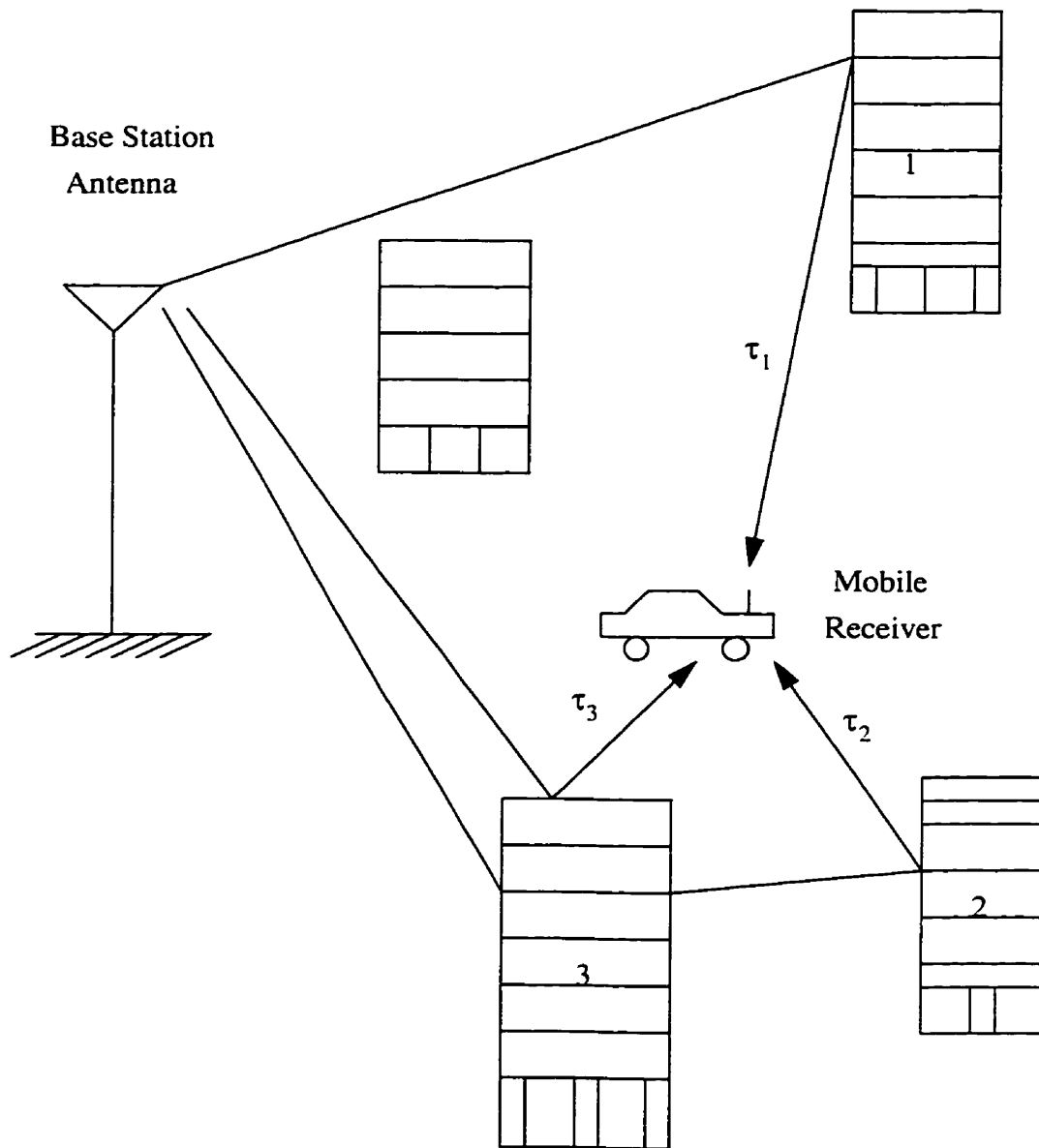


Figure 2.1 Multipath Phenomena

where $\alpha_n(t)$ and $\tau_n(t)$ are the attenuation factor and propagation delay, associated with the n th path.

Considering the Doppler shift $f_{D,n}(t)$ introduced by the vehicle movement, the attenuation factor $\alpha_n(t)$ can be written as

$$\alpha_n(t) = \alpha'_n(t) \cdot e^{j2\pi f_{D,n}(t)(t - \tau_n(t))} \quad (2.3)$$

where: $f_{D,n}(t) = f_v \cdot \cos\theta_n(t)$ (2.4)

$f_v = \frac{v}{\lambda_c}$; v is the vehicle speed; λ_c is the wavelength of the arriving plane wave;

and $\theta_n(t)$ is the angle of incidence (see Fig. 2.2).

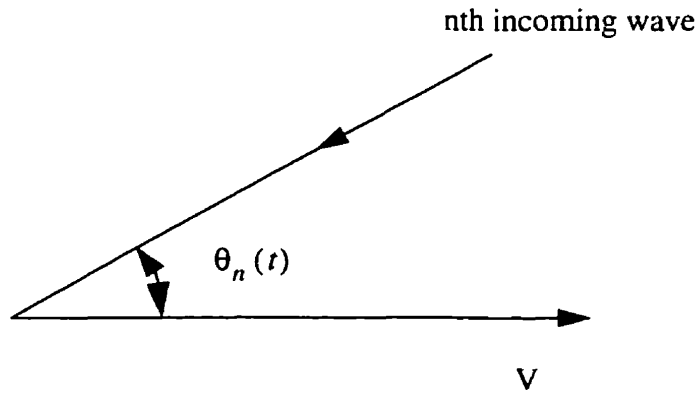


Figure 2.2 A typical plane wave component incident on a vehicle receiver [24]

If $s(t)$ of Eq(2.1) is substituted into Eq(2.2), then

$$x(t) = Re \left\{ \left[\sum_{n=1}^N \alpha_n(t) \cdot \exp(-j2\pi f_c \tau_n(t)) \cdot u(t - \tau_n(t)) \right] \cdot \exp(j2\pi f_c t) \right\}$$

$$= \text{Re} [r(t) \cdot \exp (j2\pi f_c t)] \quad (2.5)$$

where

$$r(t) = \sum_{n=1}^N \alpha_n(t) \cdot \exp (-j2\pi f_c \tau_n(t)) \cdot u(t - \tau_n(t)) \quad (2.6)$$

is the equivalent baseband complex received signal. Since the low-pass signal $r(t)$ is the response of a channel to the low-pass input signal $u(t)$, it follows that the equivalent low-pass channel can be described by the time-varying impulse response:

$$c(t, \tau) = \sum_{n=1}^N \alpha_n(t) \cdot \exp (-j2\pi f_c \tau_n(t)) \cdot \delta(t - \tau_n(t)) \quad (2.7)$$

In physical terms, $c(t, \tau)$ can be interpreted as the channel response at time t due to an impulse applied at time $t - \tau$. As attenuation factors and propagation delay are time-varying and random, $c(t, \tau)$ should be a random process. When the number of the paths N is very large, based on the central limit theorem, the received signal $r(t)$ can be modelled as a complex valued Gaussian random process. It follows that $c(t, \tau)$ is also a complex valued Gaussian random process in the t (time) variable.

There are two kinds of interesting fading channels. When a direct line-of-sight path exists between the transmitter and receiver antennas, the mean value of $r(t)$ is not equal to zero, and the received complex envelope: $z(t) = |r(t)|$ has a Ricean distribution at any time t . The channel is called a Ricean fading channel. Another fading channel is called the Rayleigh fading channel. In this case, $r(t)$ has zero mean and the complex envelope: $z(t) = |r(t)|$ has a Rayleigh distribution at any time t . Since the Rayleigh fading channel is a more severe channel, and also since it is closer to the practical situation, only the Rayleigh fading channel is studied in this thesis.

In order to characterise the multipath Rayleigh fading channel, one needs to find the correla-

tion function of the zero-mean complex Gaussian process $c(t, \tau)$. To accomplish this the following assumptions are made: 1) $c(t, \tau)$ is wide-sense-stationary (WSS); and 2) the attenuations and phase shifts associated with two path delays τ_1 and τ_2 are uncorrelated. Based on these assumptions, $c(t, \tau)$ becomes a wide-sense-stationary uncorrelated scattering (WSSUS) process and the autocorrelation function of $c(t, \tau)$ can be written as:

$$\begin{aligned}\phi_c(\Delta t, \tau_1, \tau_2) &= \frac{1}{2} \cdot E \left[c^*(t, \tau_1) \cdot c(t + \Delta t, \tau_2) \right] \\ &= \phi_c(\Delta t, \tau_1) \cdot \delta(\tau_1 - \tau_2) \quad (2.8)\end{aligned}$$

Now define

$$\Phi_c(\Delta f, \Delta t) \equiv \int_{-\infty}^{\infty} (\phi_c(\Delta t, \tau_1) \cdot \exp(-j2\pi\Delta f\tau_1)) d\tau_1 \quad (2.9)$$

Also define functions $\phi_c(\tau)$ and $\nu(\Delta t)$:

$$\phi_c(\tau) \equiv \phi_c(0, \tau) \quad (2.10)$$

$$\nu(\Delta t) \equiv \Phi_c(0, \Delta t) \quad (2.11)$$

$\phi_c(\tau)$ is called the multipath intensity profile or the delay power spectrum of the channel and the Fourier Transform of $\nu(\Delta t)$ is called the Doppler power spectrum of the channel. In physical terms, $\phi_c(\tau)$ is simply the average power output of the channel as a function of the time delay τ , and $\nu(\Delta t)$ gives a measure of time variations of the channel. Typical $\phi_c(\tau)$ and $\nu(\Delta t)$ are shown in Fig. 2.3.; also shown in the figure are their Fourier transforms.

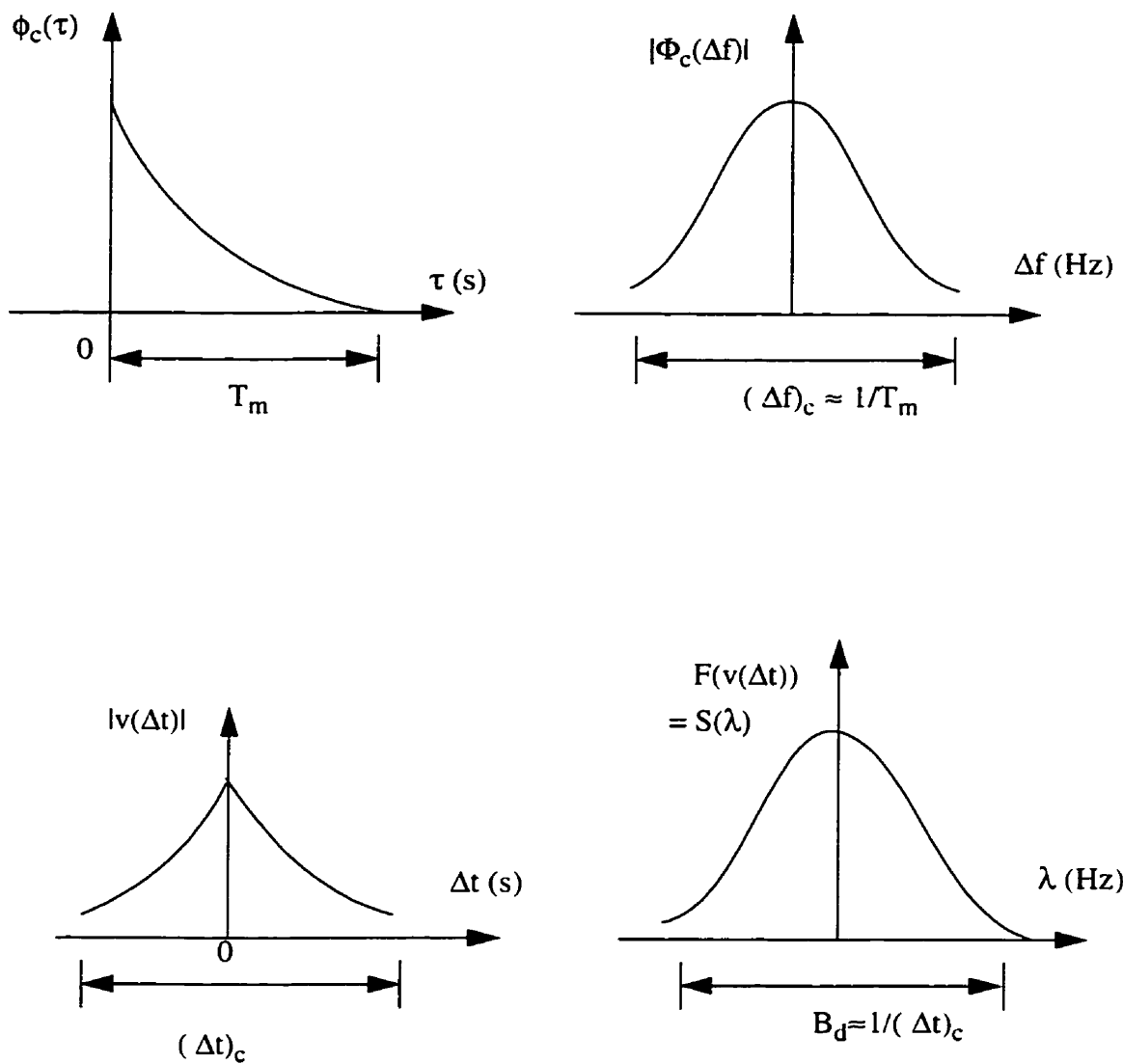


Figure 2.3 $\Phi_c(\tau)$, $v(\Delta t)$ and their Fourier transforms [22]

The figure shows two interesting parameters; T_m , the multipath spread of the channel and $(\Delta t)_c$ known as the coherence time of the channel. When T_m is greater than the signal period T , i.e. the coherence bandwidth of the channel $(\Delta f)_c$ is smaller than the bandwidth of the transmitted signal, individual frequency components of the signal experience a different fade and in this case, the channel is called a frequency selective fading channel. Depending on the relationship between $(\Delta t)_c$ and T , the channel is also classified as a slow fading channel ($(\Delta t)_c \gg T$) or a fast fading channel ($(\Delta t)_c \leq T$, $(\Delta t)_c \sim T$). This thesis studies the frequency selective Rayleigh fading channel (fast or slow).

A simplified model of a high-speed communication system is shown in Fig 2.4. For the frequency selective Rayleigh fading channel, let the length of ISI, caused by channel's band-limitation and frequency selectivity, be $L-1$, and consider the received signal $r(t)$ to be sampled at a rate T_s . Depending on the parameter α : $\alpha = \frac{T}{T_s}$ (the number of samples within each information symbol period T) and as derived in [23], the sufficient statistic r_k can be written as follows

$$\begin{aligned}
 r_k &= y_k + n_k \\
 &= \sum_{i=0}^{\beta} b_{k-i} \cdot h_{k,i} + n_k \quad (2.12)
 \end{aligned}$$

where n_k is white Gaussian noise; β is the number of correlated samples at time k ;

$L-1 = \left\lfloor \frac{\beta}{\alpha} \right\rfloor$, $\lfloor \cdot \rfloor$ is the floor function; and

$$b_k = \begin{cases} \frac{a_k}{\alpha} & \frac{k}{\alpha} \text{ an integer} \\ 0 & \text{otherwise} \end{cases} \quad (2.13)$$

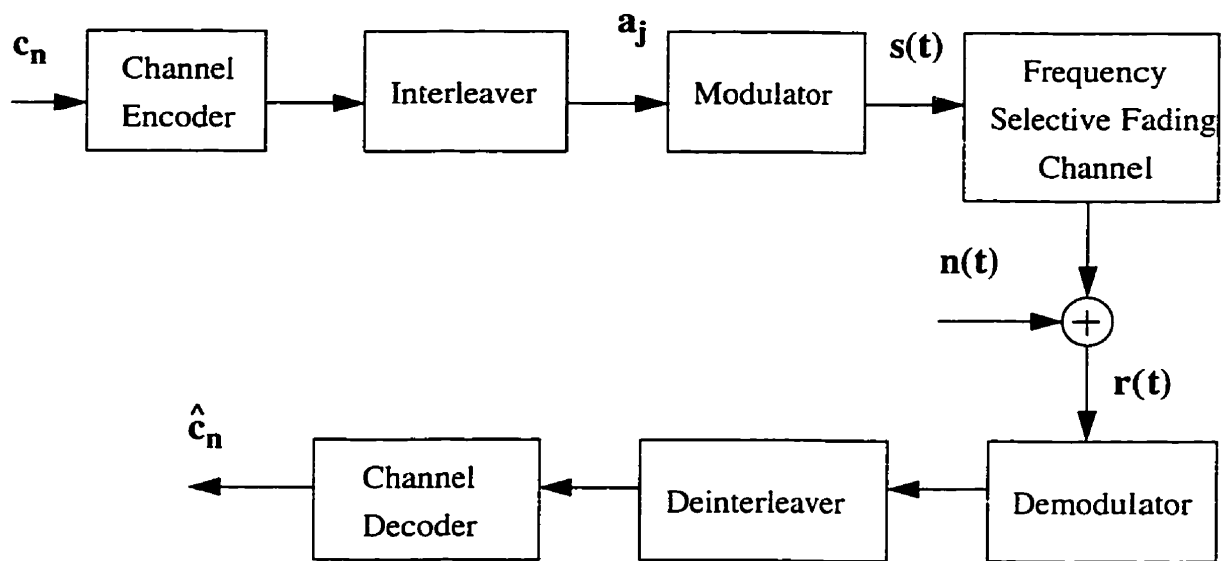


Figure 2.4 A typical digital communication system for the frequency selective Rayleigh fading channel

$$h_{k,i} = \int_{-\infty}^{\infty} c(kT_s, \lambda) \cdot f[(k-i)T_s - \lambda] d\lambda \quad (2.14)$$

Based on Eq(2.12), the frequency selective Rayleigh fading channel can be modelled with the following finite state machine model (Fig.2.5).

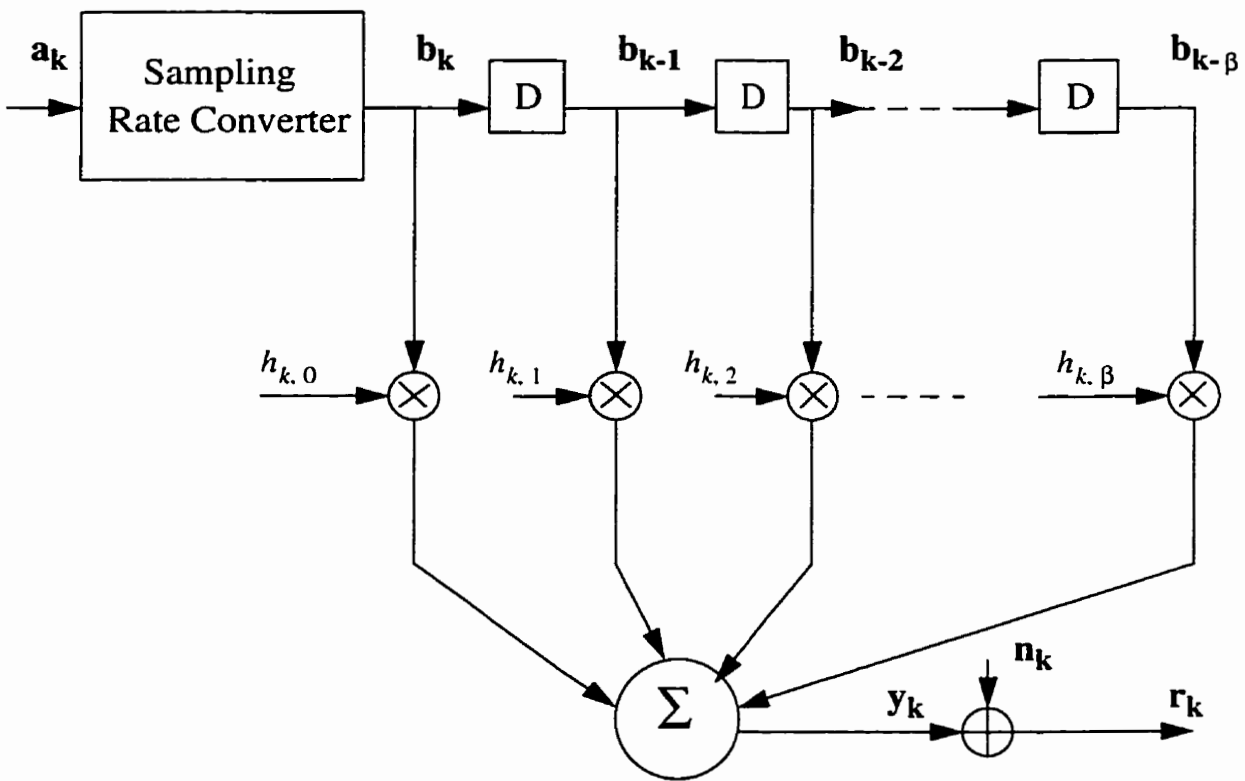


Figure 2.5 Frequency selective Rayleigh fading channel model

2.2 ARMA channel model and Kalman filter

Eq(2.12) can be written in vector form as

$$r_k = H_k^T \cdot X_k + n_k \quad (2.15)$$

where $H_k^T = (b_k, b_{k-1}, \dots, b_{k-\beta})$

$$X_k = (h_{k,0}, h_{k,1}, \dots, h_{k,\beta})^T$$

When $c(t, \tau)$ is a wide-sense-stationary (WSS) complex Gaussian random process, the channel response X_k is a WSS Gaussian random vector and can be described by the following (1,0)

ARMA model:

$$X_{k+1} = F \cdot X_k + G \cdot W_k \quad (2.16)$$

where F and G are both $(\beta + 1) \cdot (\beta + 1)$ matrices. Eq(2.15) and Eq(2.16) show that the fading process can be represented by a finite state space model as shown in Fig. 2.6.

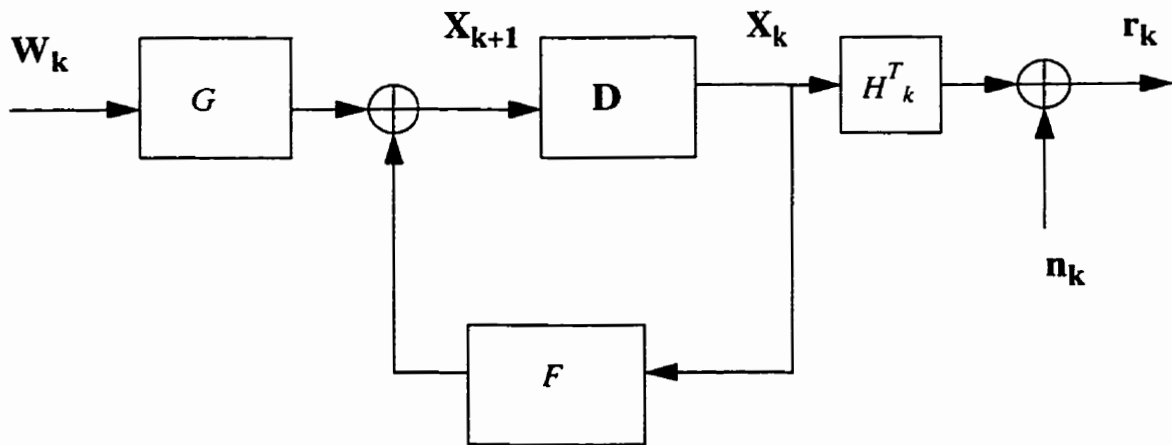


Figure 2.6 Finite state space model for the Rayleigh fading channel [23]

In figure 2.6, X_{k+1} is the state vector, F is the state transition matrix, G is the process noise coupling matrix, and W_k is a $\beta + 1$ dimensional zero mean, white, complex Gaussian vector process. Both F and G are time-variant and can be determined from second order channel statistics or by the method proposed in [25].

The object of demodulation and decoding is to detect/estimate the possible transmitted signal from the sufficient statistic r_k . In the frequency selective Rayleigh fading channel, the symbol period T is shorter than the channel multipath spread T_m , some energy will spill over from the current symbol period into the next one, and make the samples correlated. In order to remove this correlation (whiten r_k), the receiver needs to estimate the channel impulse response. Many methods have been proposed to estimate the CIR, but for the frequency selective Rayleigh fading channel, especially for fast fading, most of these methods break down. Thus the Kalman filter, an optimal linear minimum variance estimator, is introduced to solve this problem.

The principle of using the Kalman filter to estimate CIR is simple. If the state space equations (2.15) and (2.16) are rewritten as follows:

$$\begin{cases} X_{k+1} = F \cdot X_k + G \cdot W_k \\ r_k = H_k^T \cdot X_k + n_k \end{cases}$$

Then it is readily seen that they represent a Kalman filtering problem. The solution is a Kalman filter [26]:

$$\begin{aligned} \widehat{X}_{k+1} &= [F - K_k H_k^T] \cdot \widehat{X}_k + K_k r_k \\ K_k &= F \Sigma_k H_k \cdot [H_k^T \Sigma_k H_k + N_0]^{-1} \\ \Sigma_{k+1} &= [F - K_k H_k^T] \Sigma_k F^T + G G^H \end{aligned} \quad (2.17)$$

where \widehat{X}_k is the estimate of the state vector X_k .

Therefore, after finding the matrices F, G, for every received signal r_k and hypothesised vector H_k , the Kalman filter provides a CIR \widehat{X}_k , which is used to calculate the conditional mean

$\bar{r}_k(m)$ and variance $\sigma_k^2(m)$:

$$\bar{r}_k(m) = H_k^T \cdot \widehat{X}_k \quad (2.18)$$

$$\sigma_k^2(m) = H_k^T \Sigma_k H_k + N_0 \quad (2.19)$$

Finally the optimal log-likelihood metric used in MLSE-VA is given by [23]

$$\Lambda_N^m(r) = \sum_{k=1}^{\alpha N} \left\{ \frac{|r_k - \bar{r}_k(m)|^2}{\sigma_k^2(m)} + \log [\sigma_k^2(m)] \right\} \quad (2.20)$$

The typical MLSE-VA receiver for the frequency selective Rayleigh fading channel is shown in Fig.2.7.

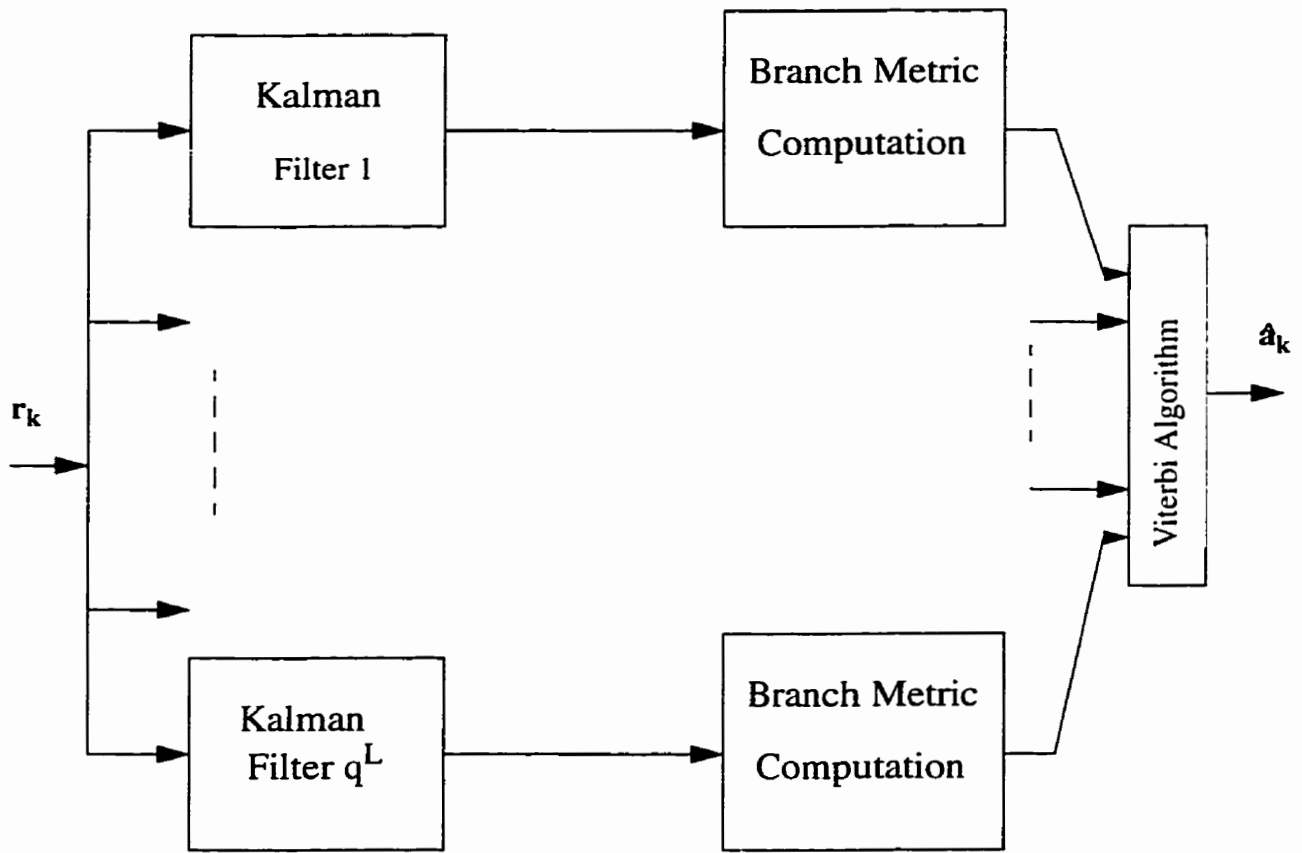


Figure 2.7 The MLSE-VA receiver for the frequency selective Rayleigh fading channel [16]

Chapter 3

Symbol-by-symbol MAP joint demodulation and decoding

A MLSE receiver for the frequency selective Rayleigh fading channel has been proposed by Dai and Shwedyk in [16], where optimal demodulation and decoding are performed in one stage, i.e. the Viterbi Algorithm searches a composite trellis which combines the channel memory and coding memory. One disadvantage is noticed. When coding and channel memory is large, especially when there are some interleavers between the encoders, or the encoder and modulator (e.g. see Fig. 1.1), the composite trellis is usually so complex that the proposed MLSE receiver is impractical. In order to solve this problem, a suboptimal two stage receiver was proposed by Kong and Shwedyk [27](see Fig.3.1), where the receiver contains two parts, the lower part is the conventional two stage soft decision receiver and the upper part improves the first stage soft output in the lower part through channel estimation using the hard output from the second stage of lower part. A Kalman channel smoother is also used in this part. Since the hard output from the second stage is more reliable, it will generate a better channel estimate. Because this receiver feeds back only the hard output of the second stage, some useful information may be lost during the iteration.

The symbol-by-symbol maximum a posterior probability (MAP) algorithm [28], an optimal decoding algorithm, can use a priori information and also produce optimal soft output information. With this property, iterative decoding processing can be realized with the MAP algorithm, as

is done in [19-20]. Recently, Gertsman and Lodge applied the iterative processing technique to joint demodulation and decoding of the CPM signal over the Rayleigh flat-fading channel [21]. A multiple-stage receiver is proposed there and a MAP demodulator and a MAP decoder are used to demodulate and decode the signal.

In this chapter, the approaches of Gertsman and Dai are used and extended to the frequency selective Rayleigh fading channel. The Kalman filter is used to estimate the channel CIR, and the MAP demodulator and decoder/filter [29] is used to generate the necessary soft-output information. Finally iterative processing is performed to improve the final detection.

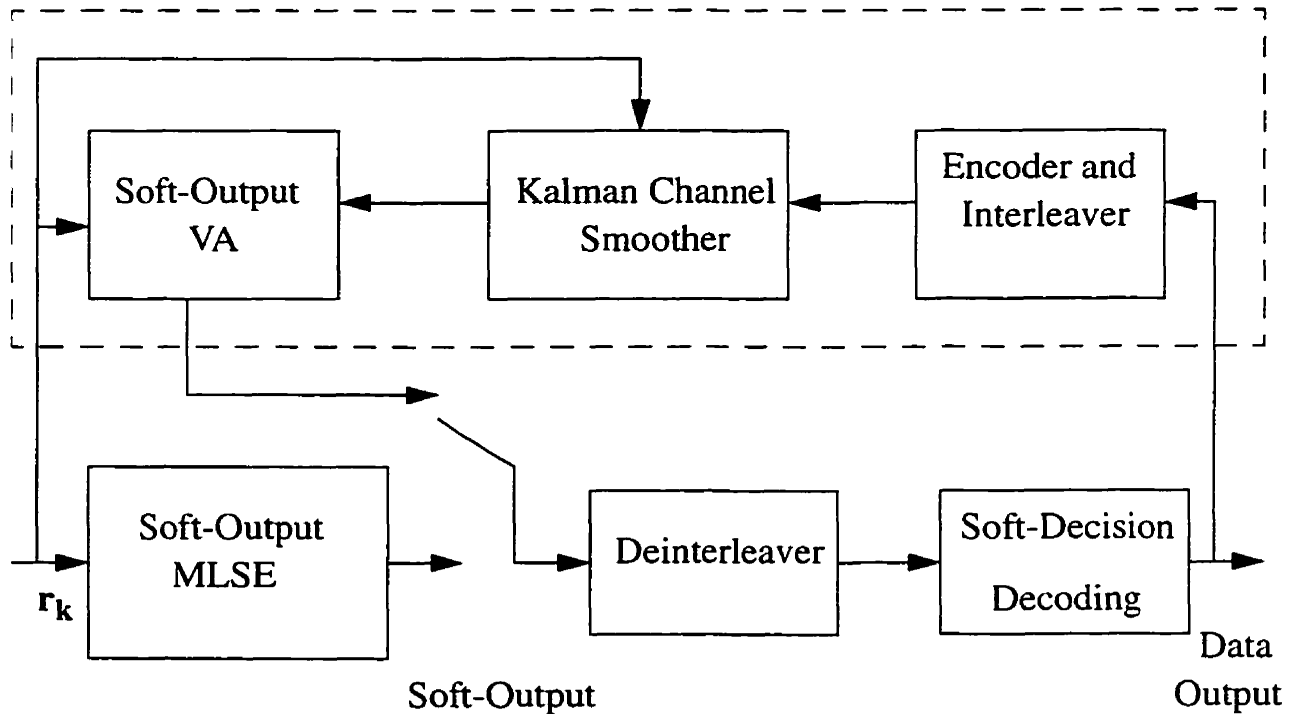


Figure 3.1 Iterative Receiver for frequency selective fading channels [27]

3.1 Symbol-by-symbol MAP demodulation

As discussed in chapter 2, when the memory of a frequency selective Rayleigh fading channel is finite, it can be represented by a finite state machine model (Fig. 2.5). Based on this model, a finite state trellis can be obtained. Figure 3.2 gives an example for a binary sequence $\{b_k\}$, channel memory $\beta = 4$ and an over sampling rate $\alpha = 2$. Based on this trellis, the symbol-by-symbol MAP algorithm is used to find the a posterior probability and soft output of every symbol as follows.

Define the soft-value $L[a_k|r_1^{\alpha N}]$ as follows:

$$L[a_k|r_1^{\alpha N}] \equiv \log \frac{p[a_k=1|r_1^{\alpha N}]}{p[a_k=0|r_1^{\alpha N}]} \quad (3.1)$$

Then the soft output L_c^r , can be written as [30]

$$L_c^r = L[a_k|r_1^{\alpha N}] - L(a_k) \quad (3.2)$$

L_c^r is also called extrinsic information in some papers [19-20,31]. When the information symbol a_k is equally likely, $L(a_k) = 0$ and $L_c^r = L[a_k|r_1^{\alpha N}]$

In order to calculate the soft value $L[a_k|r_1^{\alpha N}]$, the conditional probability $p[a_k = q|r_1^{\alpha N}]$ ($q = 0,1$) must be known.

Let:

$$\mathfrak{S} = (s_1, s_2, \dots, s_{k-1}, s_k, \dots, s_N)$$

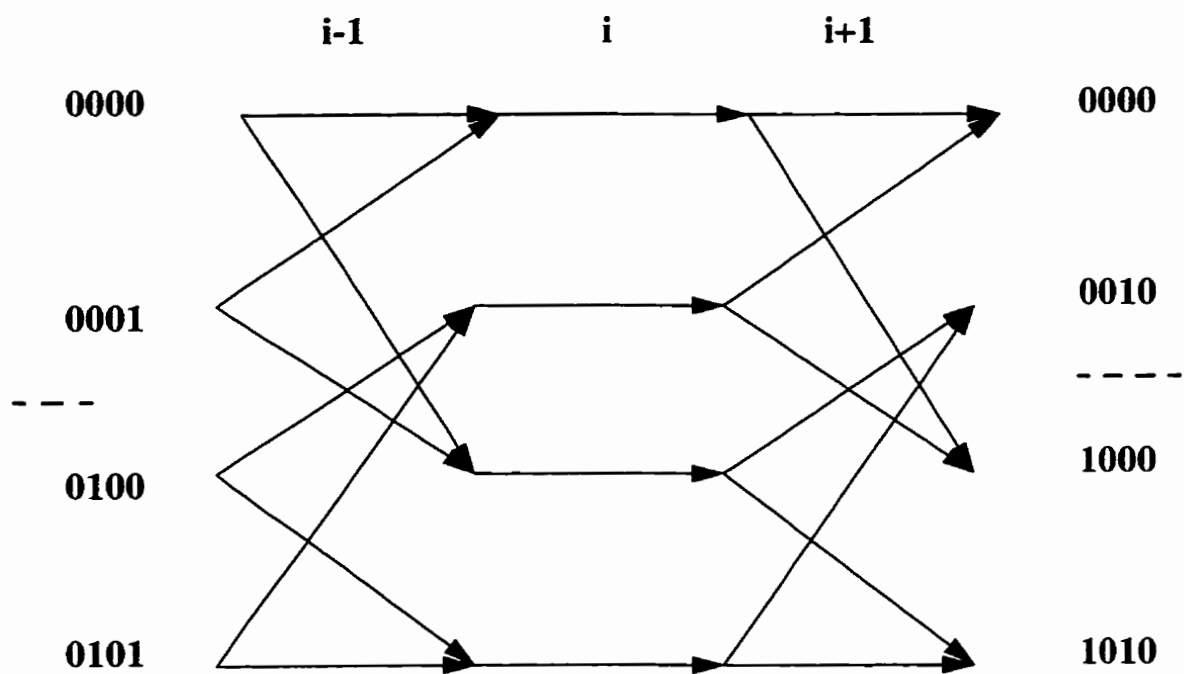


Figure 3.2 Trellis for fading channel with memory β and input $\{b\}$

be a state sequence and define set A, a set of state sequences, as follows:

$$A \equiv \{\mathcal{S}; a_k(m', m) = q, s_{k-1} = m', s_k = m\} \quad (3.3)$$

where function $a_k(m', m)$ is the corresponding coded bit (channel input) at time k, which is

present on the branch from state m' to m . The conditional probability $P[a_k = q | r_1^{\alpha N}]$ is the sum of the probabilities of all possible state sequences passing through the trellis branch between state m' and m . Hence:

$$P[a_k = q | r_1^{\alpha N}] = \sum_{\mathcal{S} \in A} P[\mathcal{S} | r_1^{\alpha N}] \quad (3.4)$$

Based on all possible (m', m) , set A can be partitioned into different disjoint subsets

$B_k(m', m)$ as

$$A = \bigcup_{(m', m) \in C} B_k(m', m) \quad (3.5)$$

where $C = \{(m', m); a_k(m', m) = q\}$

$$B_k(m', m) = \{\mathcal{S}; a_k(m', m) = q, s_{k-1} = m', s_k = m, (m', m) \text{ fixed}\}$$

Therefore

$$\begin{aligned} P[a_k = q | r_1^{\alpha N}] &= \sum_{\mathcal{S} \in A} P[\mathcal{S} | r_1^{\alpha N}] \\ &= \sum_{(m', m) \in C} \sum_{\mathcal{S} \in B_k(m', m)} P[\mathcal{S} | r_1^{\alpha N}] \\ &= \sum_{(m', m) \in C} \sum_{\mathcal{S} \in B_k(m', m)} P[a(\mathcal{S}) | r_1^{\alpha N}] \end{aligned} \quad (3.6)$$

where $a(\mathcal{S})$ is the channel input sequence corresponding to the state sequence \mathcal{S} .

Since

$$P[a(\mathcal{S}) | r_1^{\alpha N}] = \frac{P[r_1^{\alpha N} | a(\mathcal{S})] \cdot P(a(\mathcal{S}))}{P[r_1^{\alpha N}]} \quad (3.7)$$

and

$$\begin{aligned} P[r_1^{\alpha N} | a(\mathcal{S})] &= p[(r_1, r_2, \dots, r_{\alpha N}) | a(\mathcal{S})] \\ &= \prod_{i=1}^{\alpha N} P[r_i | Y_{i-1}(\mathcal{S})] \end{aligned} \quad (3.8)$$

where $Y_{i-1}(\mathcal{S}) = \{(r_{i-1}, r_{i-2}, \dots, r_1), a(\mathcal{S})\}$

Then

$$P[a(\mathcal{S}) | r_1^{\alpha N}] = K \cdot \prod_{i=1}^{\alpha N} P[r_i | Y_{i-1}(\mathcal{S})] \cdot \prod_{i=1}^N P(a_i) \quad (3.9)$$

where, $K = \frac{1}{P[r_1^{\alpha N}]}$

From [26] and [16], it is known that the probability $P[r_i | Y_{i-1}(\mathcal{S})]$ is a complex Gaussian density function, and can be written as

$$P[r_i | Y_{i-1}(\mathcal{S})] = \frac{1}{\sqrt{2\pi\sigma_i^2(\mathcal{S})}} \cdot \exp\left\{-\frac{|r_i - \bar{r}_i(\mathcal{S})|^2}{2\sigma_i^2(\mathcal{S})}\right\} \quad (3.10)$$

where

$$\bar{r}_i(\mathcal{S}) = E\{r_i | Y_{i-1}(\mathcal{S})\}$$

$$\sigma_i^2(\hat{S}) = E\{[r_i - \bar{r}_i(\hat{S})]^2 | Y_{i-1}(\hat{S})\}$$

$\bar{r}_i(\hat{S})$ and $\sigma_i^2(\hat{S})$ are provided by the Kalman filter.

Define $\gamma_j(m', m)$, the branch weight from m' to m at time j , as

$$\gamma_j(m', m) = \prod_{i=\alpha_j}^{\alpha(j+1)-1} P[r_i | Y_{i-1}(\hat{S})] \cdot P(a_j) \quad (3.11)$$

Combine Eq(3.6)-(3.11), to obtain

$$p[a_k = q | r_1^{\alpha N}] = K \cdot \sum_{(m', m) \in C} \sum_{\hat{S} \in B_k(m', m)} \prod_{j=1}^N \gamma_j(m', m) \quad (3.12)$$

Following reference [28], let

$$\alpha_k(m) = \sum_{m'} \alpha_{k-1}(m') \cdot \gamma_k(m', m) \quad (3.13)$$

$$\beta_k(m) = \sum_{m'} \beta_{k+1}(m') \cdot \gamma_{k+1}(m, m') \quad (3.14)$$

and

$$\sigma_k(m', m) = \alpha_{k-1}(m') \cdot \gamma_k(m', m) \cdot \beta_k(m) \quad (3.15)$$

Then

$$\sum_{\hat{S} \in B_k(m', m)} \prod_{j=1}^N \gamma_j(m', m) = \sigma_k(m', m) \quad (3.16)$$

Finally

$$p[a_k = q | r_1^{\alpha N}] = K \cdot \sum_{(m', m) \in C} \sigma_k(m', m) \quad (3.17)$$

The soft-value $L[a_k | r_1^{\alpha N}]$ then can be expressed as

$$L[a_k | r_1^{\alpha N}] = \log \frac{\sum_{(m', m) \in C_1} \sigma_k(m', m)}{\sum_{(m', m) \in C_2} \sigma_k(m', m)} \quad (3.18)$$

where $C_1 = \{(m', m) ; a_k(m', m) = 1\}$

$C_2 = \{(m', m) ; a_k(m', m) = 0\}$

Now considering the trellis structure of Fig. 3.2, it can be seen that, at time i , there is only one branch output from each state. For each of these branches, a Kalman filter is used to estimate \widehat{X}_i , the channel impulse response. Consider state (0000). Since two branches enter this state at time $i-1$, two possible \widehat{X}_{i-1} are generated. Which one should be chosen as the initial condition for estimating \widehat{X}_i ? A natural way to do this is to choose the one with the largest partial metric. This method is used in this chapter.

Hence, the symbol-by-symbol MAP demodulation can be realized by the following steps:

step1): initialize X_0 , Σ_0 , $\alpha_0(m)$ and $\beta_N(m)$:

$$X_0 = [0] \quad ; \quad \Sigma_0 = R(0)$$

$$\alpha_0(0) = 1 \quad ; \quad \alpha_0(m) = 0 \quad ; \quad \text{for } m \neq 0$$

$$\beta_N(0) = 1 \quad ; \quad \beta_N(m) = 0 \quad ; \quad \text{for } m \neq 0$$

step 2): for $i=1$ to αN ($j=1$ to N):

a) use the Kalman filter to estimate the CIR;

b) calculate $\widehat{r}_i(\hat{\mathcal{S}})$, $\sigma_i^2(\hat{\mathcal{S}})$ and $P[r_i | Y_{i-1}(\hat{\mathcal{S}})]$;

c) compute $\gamma_j(m', m)$;

d) calculate the branch metric and the partial metric for all the paths entering a state. For each state, store the CIR with the largest metric which will be used by the Kalman filter to estimate the CIR at the next time interval.

e) if $i < \alpha N$, goto a); otherwise goto step 3);

step 3) using Eq(3.13) - Eq(3.15), compute, $\alpha_j(m)$, $\beta_j(m)$ and $\sigma_j(m', m)$;

step 4): obtain LLR(a_j) and $L_c^r(a_j)$.

The corresponding receiver structure is given in Fig.3.3.

3.2 Joint demodulation and decoding with iterative MAP processing

Recent research has shown that substantial coding gain can be obtained by the iterative MAP processing technique. Interesting work has been done by Benedetto and Montorsi [32-33], where they decoded serially concatenated convolutional codes with the iterative MAP processing technique. The serially concatenated convolutional codes and its decoder are shown in Fig. 3.4.

Since, as discussed in chapter 2, the shaping filter and frequency selective Rayleigh fading channel can be represented by a finite state machine model (as shown in Fig.2.5), to a certain extent, they can be treated as a special encoder. Therefore, the encoder, shaping filter and channel can be modelled as an equivalent serially concatenated coder(Fig 3.5).

In Fig 3.5, encoder II contains the influence of the shaping filter and fading channel. Fig 3.5 and Fig.3.4 (a) have a similar structure, thus the decoding method processed in [32] can be extended

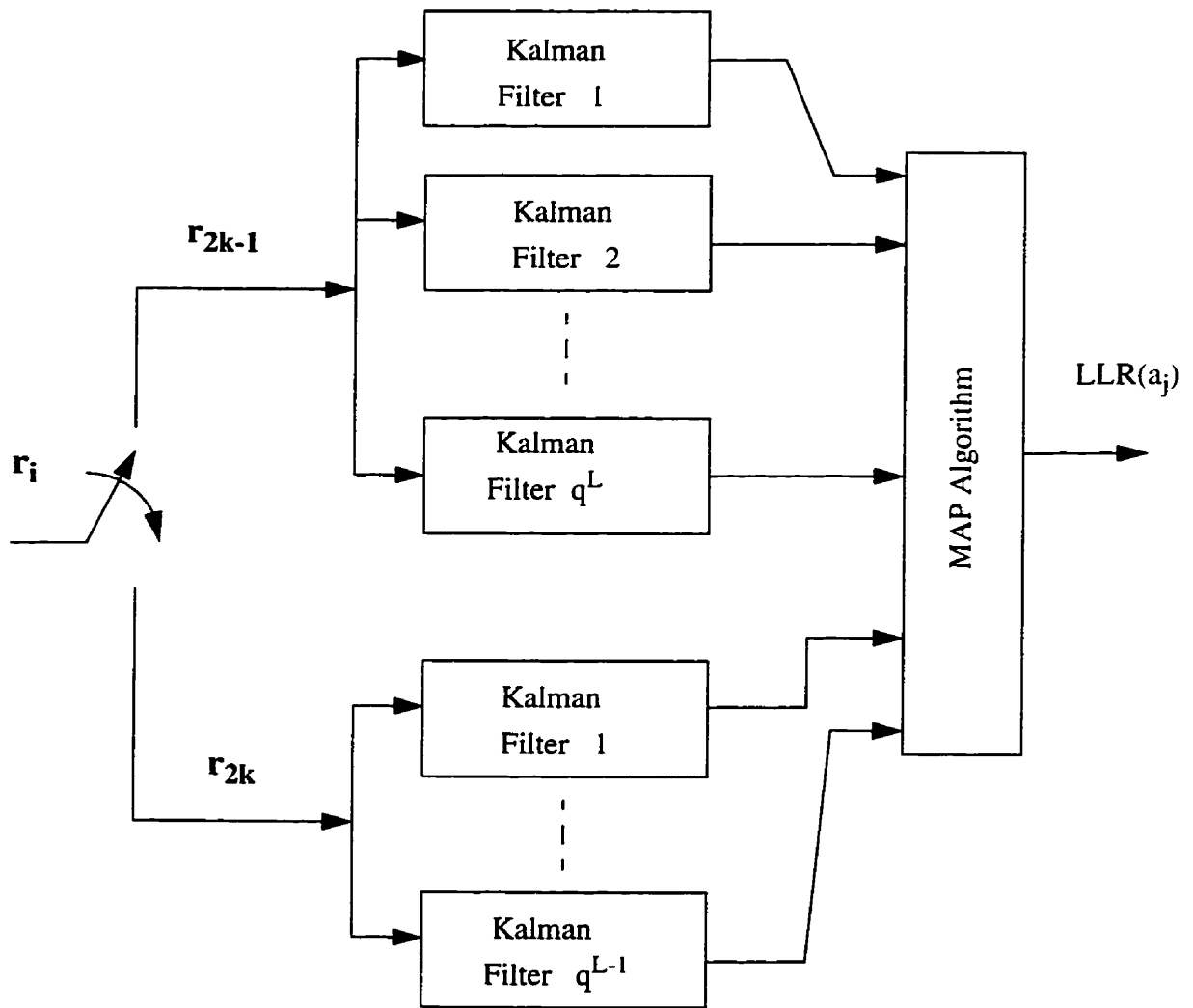
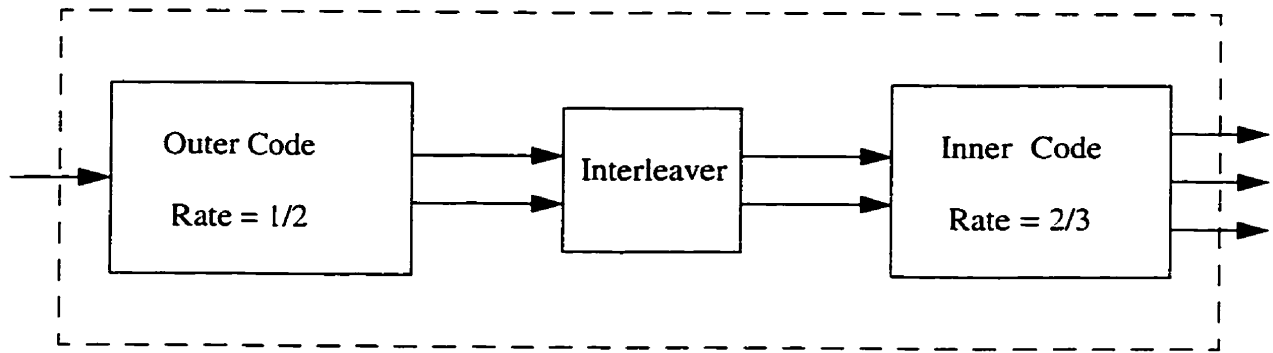
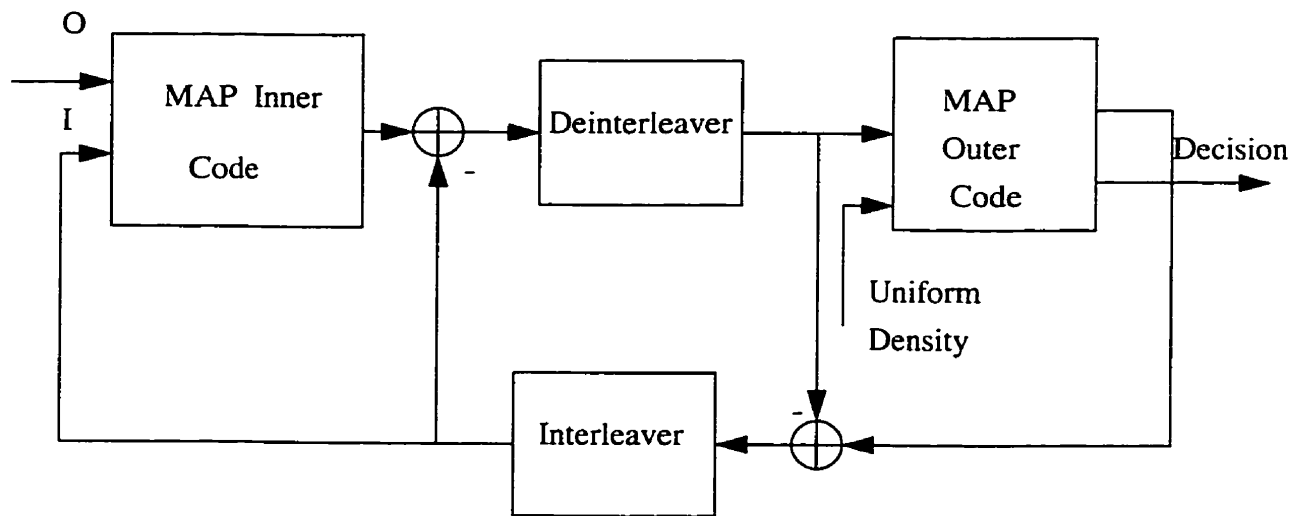


Figure 3.3 MAP demodulator for frequency selective Rayleigh fading channels

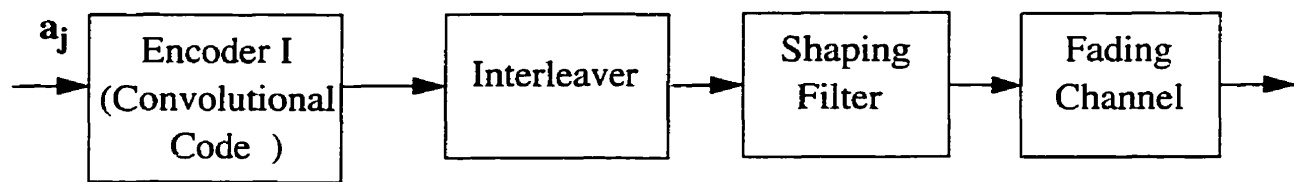


(a)

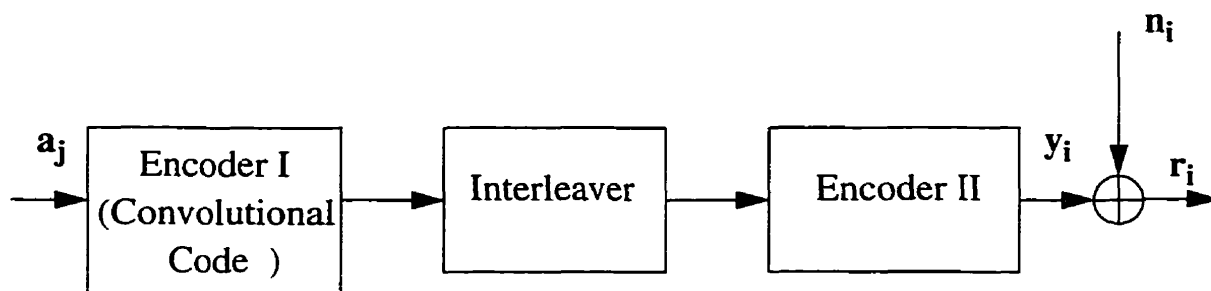


(b)

Figure 3.4 Serially concatenated convolutional code and its iterative decoder [32]
 (a) encoder; (b) Iterative decoding algorithm



(a)



(b)

Figure 3.5 Digital transmission system (a) and its equivalent serially concatenated encoder for convolutional encoder, interleaver and frequency selective fading channel (b)

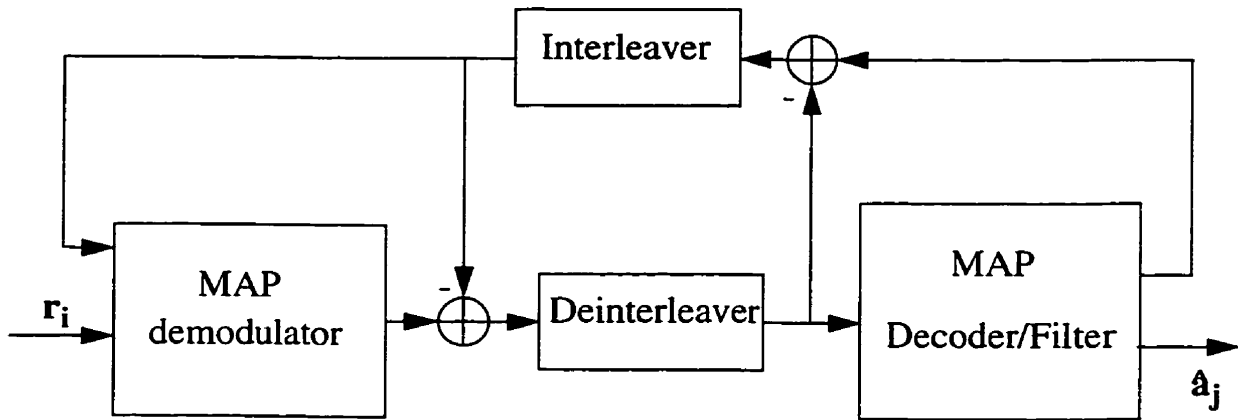


Figure 3.6 Iterative MAP demodulation and decoding algorithm for frequency selective Rayleigh fading channel

and applied to iterative demodulation and decoding the signals over the frequency selective Rayleigh fading channel. Fig 3.6 gives the iterative MAP demodulation and decoding structure used in this thesis.

3.3 Simulation Results

In this section, a computer simulation has been done for a frequency selective Rayleigh fading channel where the channel model used is exactly the same as the one used in [23] with an autocorrelation function given by

$$\phi_c(\tau_1, \tau_2, \Delta t) = A \exp[-a\tau_1^2] \cdot \exp\left[-b \cdot \frac{|\Delta t|}{T}\right] \cdot \delta(\tau_1 - \tau_2) \quad (3.19)$$

The parameters are $a = 0.6$, $L-1 = 4$. Depending on the two different values of normalized Doppler frequency parameter b , slow and fast fading have been studied. The shaping filter was chosen to be

$$f(t) = \frac{\cos 2\pi t}{1 - 16t^2} \quad (3.20)$$

The state transition matrix F and noise coupling matrix G can be calculated from the autocorrelation matrix $R(0)$ as

$$F = R(0) \cdot R(0)^{-1} = e^{-b \cdot \frac{|T_s|}{T}} \cdot I \quad (3.21)$$

$$G \cdot G^+ = \left[1 - e^{-2b \cdot \frac{|T_s|}{T}} \right] \cdot R(0) \quad (3.22)$$

where

$$R(0) = \frac{1}{2} \cdot E\{h_k \cdot h_k^H\} = \{r_{ij}\}$$

and $r_{ij} = \int (f(iT_s - \lambda) \cdot f(jT_s - \lambda) \cdot \phi_c(ms; \lambda)) d\lambda \quad i, j = 0, 1, 2, \dots, \beta$

The initial conditions for each Kalman filter are identical and are chosen as follows:

$$\hat{X}_0 = [0] \quad (3.23)$$

$$\Sigma_1 = R(0) \quad (3.24)$$

Finally, the definition of SNR used in this thesis is the same as that in [23] :

$$SNR = \frac{Var(h_{k,0})}{N_0} \quad (3.25)$$

Fig.3. 7 shows the block diagram of the simulation, where the binary random sequence is generated by a pseudo-random generator. The length of sequence used varied with the SNR and is divided into frames of 128 bits. The interleaver used in simulation is a 8x16 block interleaver. A sampling rate convertor is used to change the transmission symbol spacing from T to $T_s=T/2$ (the channel sample spacing), by inserting zeros between each data symbol entering the channel. In this case, the oversampling factor $\alpha = \frac{T}{T_s} = 2$ (the number of samples in each symbol interval T) is obtained. Based on the (1,0) ARMA model, the shaping filter and frequency selective Rayleigh fading channel is modelled as a FIR filter with complex Gaussian taps. The demodulation and decoding algorithms are given in the previous section. Finally, an error counter is used to compute an error rate by comparing the bit stream detected by the receiver with that sent to the encoder.

The simulations were done on Sun stations in the language C++ over a SNR range of 5-20 dB. Two different fading rates, $b = 0.05$, and $b = 0.005$, are used in the simulations. Under the assumption of a signalling rate of 24Kbits/s and a carrier frequency of 900 MHz, these values correspond to vehicle speeds of 200Km/h and 20Km/h, respectively.

Fig. 3.8 shows the bit error probabilities (BER) of MAP demodulation for the frequency selective Rayleigh fading channel. The convolutional encoder and interleaver are not used in this simulation. Fig. 3.9 gives the BER for MAP demodulation and decoding with the (2,1,5) convolution code and an interleaver. The error performance of the iterative MAP receiver when convolutional codes and an interleaver are used is given in Fig. 3.10 and Fig. 3.11. Up to 2 iterations have been performed and the results indicate that significant gain can be obtained with the first iteration.

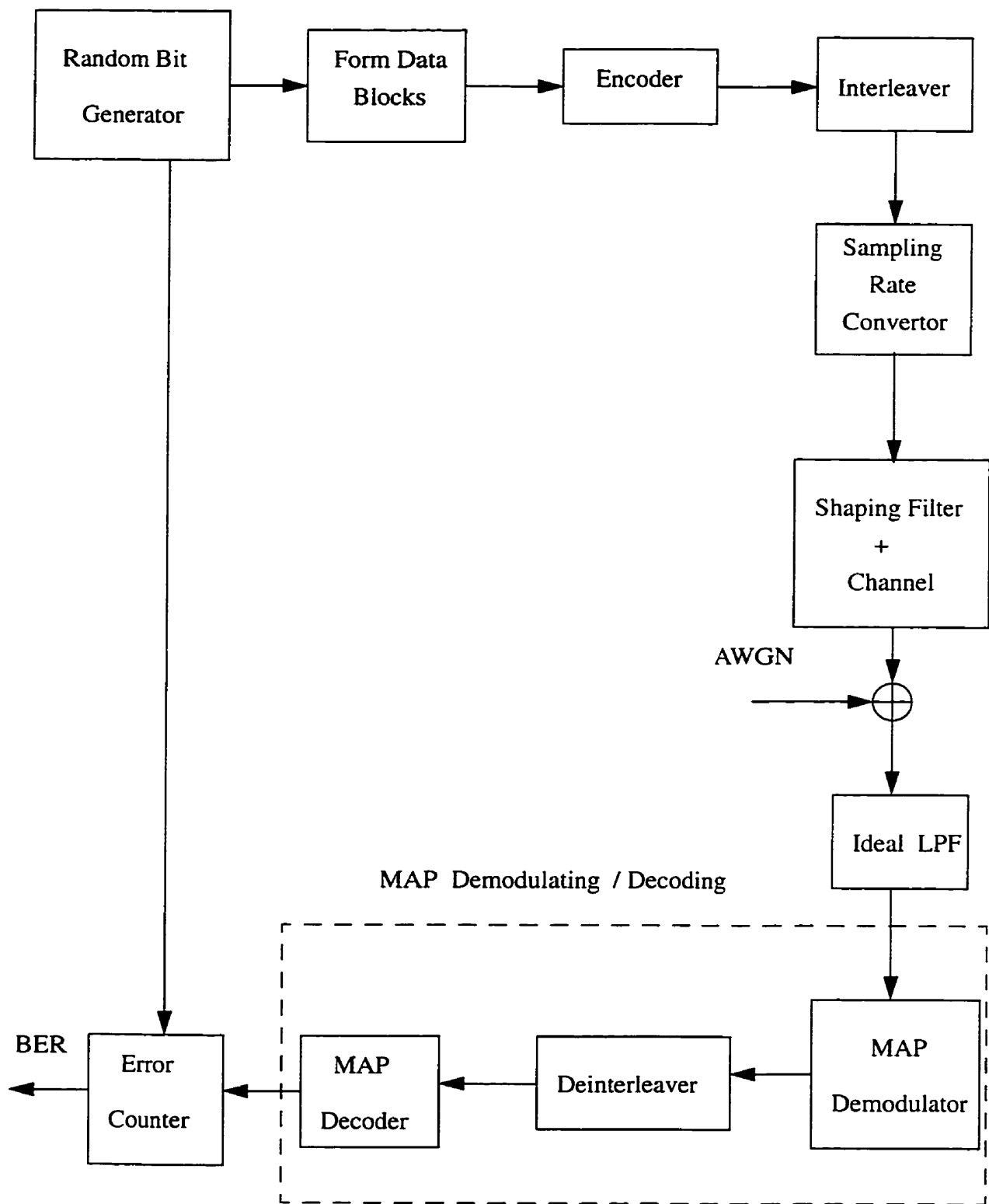


Figure 3.7 Simulation Block Diagram

3.4 Summary

An iterative MAP receiver for joint demodulation and decoding of signals transmitted over the frequency selective Rayleigh fading channel has been studied in this chapter. First a symbol-by-symbol MAP demodulation algorithm is derived by following the BCJR algorithm and Dai's [28,16] approach. Compared to previously proposed receiver structures used for the same type of fading channel, an important feature of the MAP receiver is that soft information (soft decision) is generated at the output of the MAP demodulator. This makes it possible to use it in the applications where the subsequent stages require a soft decision from the demodulator.

In order to obtain near-optimal performance, the Benedetto and Montorsi approach is extended and an iterative MAP receiver is developed in section 2. Its error performance is studied by computer simulation in section 3. The results indicate that a coding gain of 3dB can be achieved at a bit error rate level of 10^{-3} for a slowly fading channel after the first iteration (Fig. 3.10). For the fast one, the BER changes from 10^{-2} to 6×10^{-3} at 10dB and from 3×10^{-2} to 8×10^{-3} at 15dB with the first iteration (Fig. 3.11).

It is well known, that the MAP algorithm is complex with respect to computation, especially when the size of interleaver is large. The results for turbo codes indicate that a large interleaver usually improves the BER performance. Therefore it is interesting to study a soft-in, soft-out algorithm which is simpler than the MAP algorithm but can be applied to a large interleaver size. That is the subject of chapter 4.

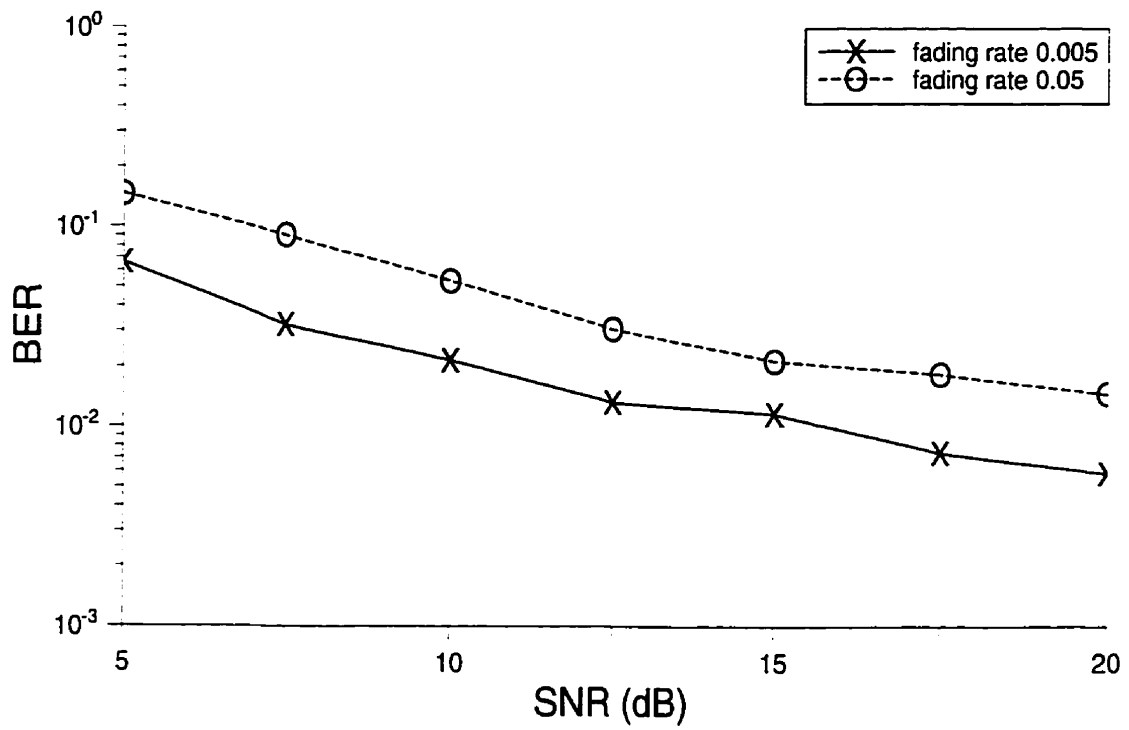


Figure 3.8 BER performance of MAP demodulation for the frequency selective Rayleigh fading channel

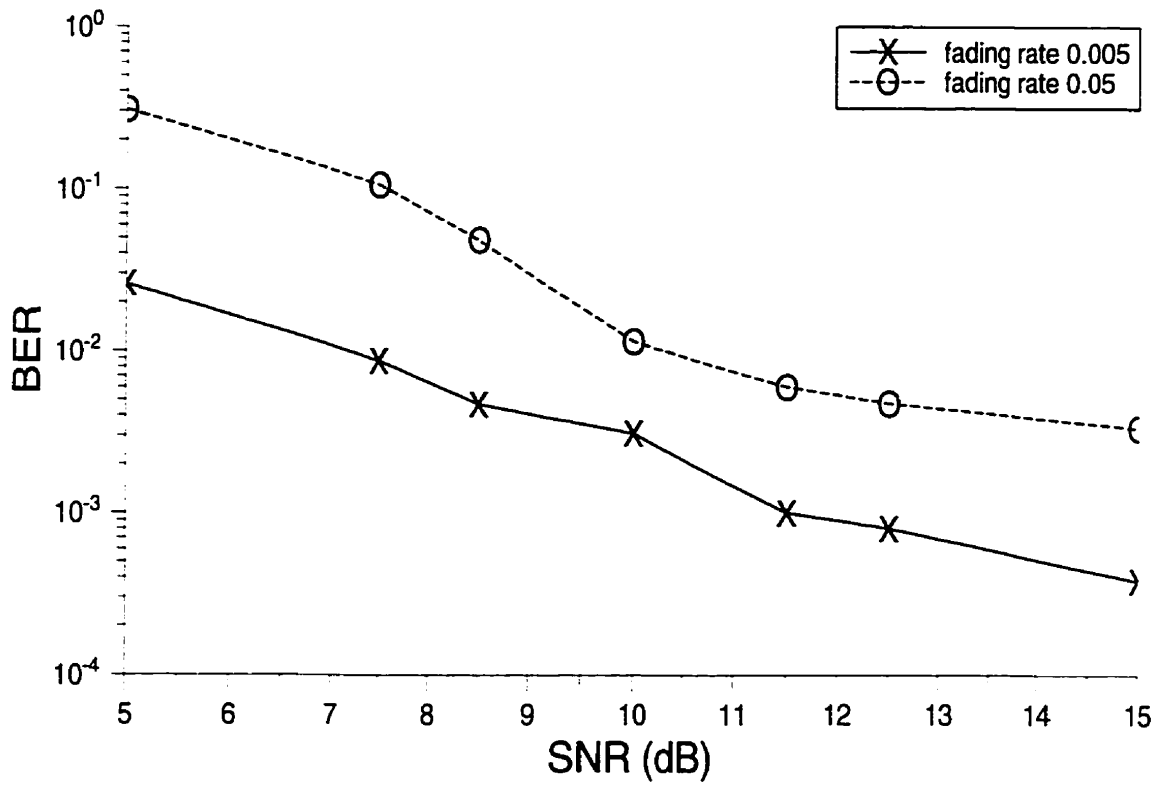


Figure 3.9 BER performance of MAP demodulation and decoding for the frequency selective Rayleigh fading channel

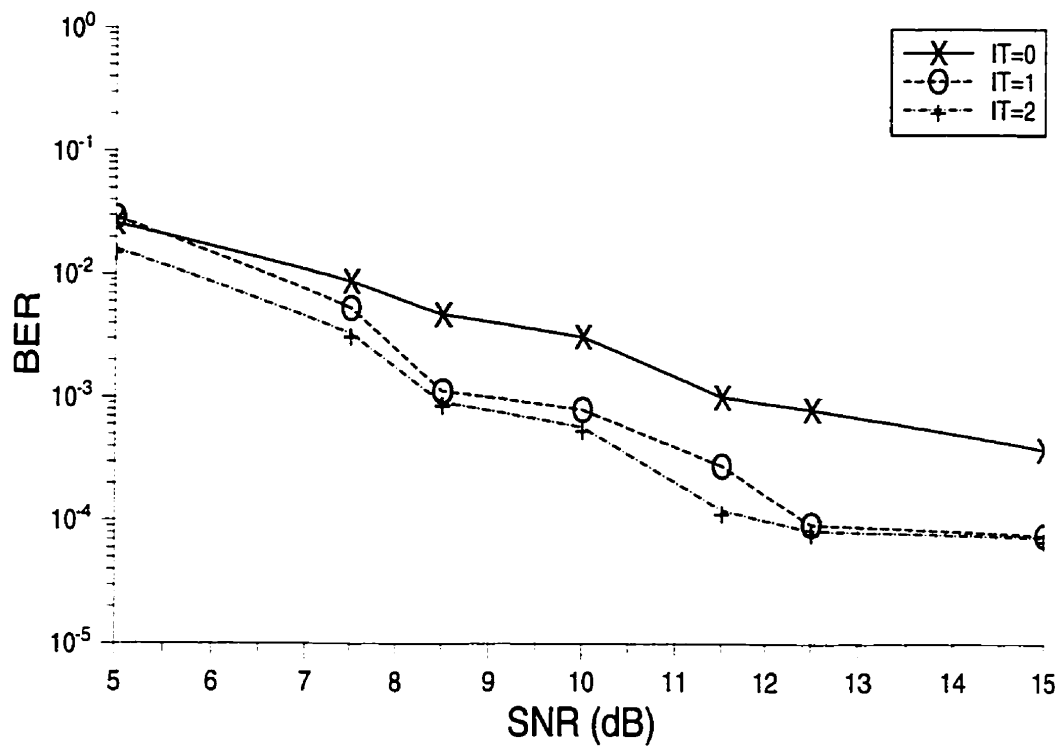


Figure 3.10 BER performance of the iterative MAP receiver for a slow fading channel. IT=0 means no iteration is performed, while IT=1 and IT=2 denote the 1st and 2nd iteration.

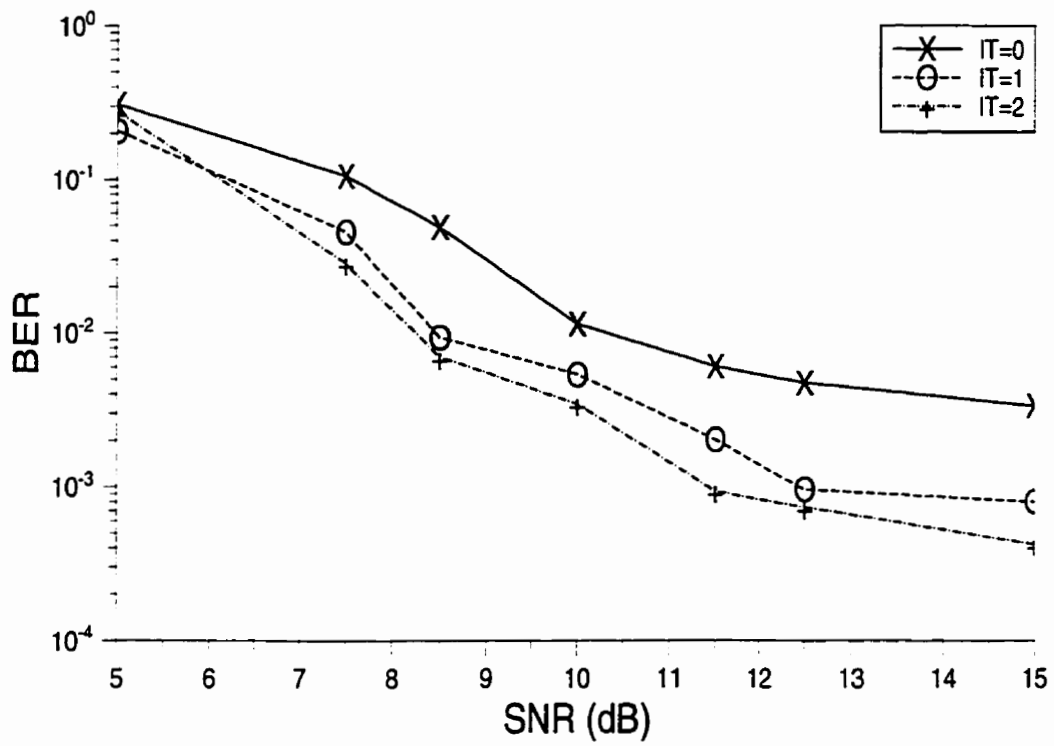


Figure 3.11 BER performance of iterative MAP receiver for a fast fading channel
 IT=0 means no iteration is performed, while IT=1 and IT=2 denote
 the 1st and 2nd iteration.

Chapter 4

Joint demodulation and decoding with Apri-SOVA algorithm

The symbol-by-symbol MAP algorithm is an optimal decoding algorithm, but it is too difficult to realize in practice, basically because of the numerical representation of probabilities, nonlinear functions and mixed multiplications and additions of these values [34]. In order to solve these problems and simplify the receiver structure, the Apri Soft-Output Viterbi Algorithm (Apri-SOVA) [35,30] is applied in this chapter. As Apri-SOVA looks at only two paths per step (the best paths with bit one and zero at transmission time k), while MAP takes all paths into its calculation, the complexity of Apri-SOVA must be much simpler compared to MAP. Also in Apri-SOVA, a sliding-window method is used, therefore a large size interleaver can be used without increasing the computational complexity. The structure of Apri-SOVA receiver for the frequency selective Rayleigh fading channel is shown in Fig 4.1.

4.1 Apri-SOVA demodulation

As discussed in chapter 3, when the fading channel contains finite memory, it can be represented by a finite state trellis and Apri-SOVA can be applied to find the soft-output information of the possible transmitted bits. The Apri-SOVA algorithm has been studied by Hagenauer, Rober-

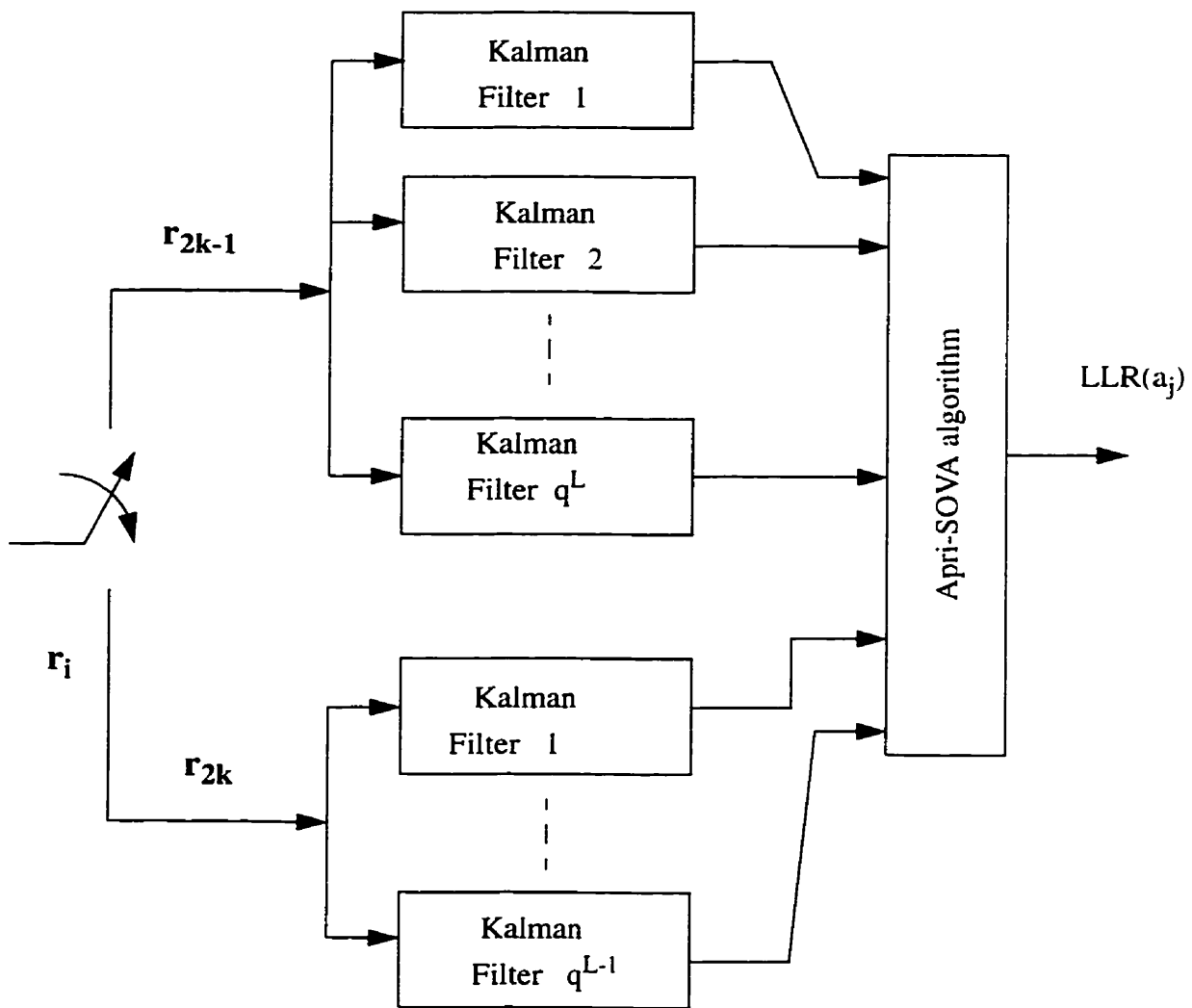


Figure 4.1 (a)

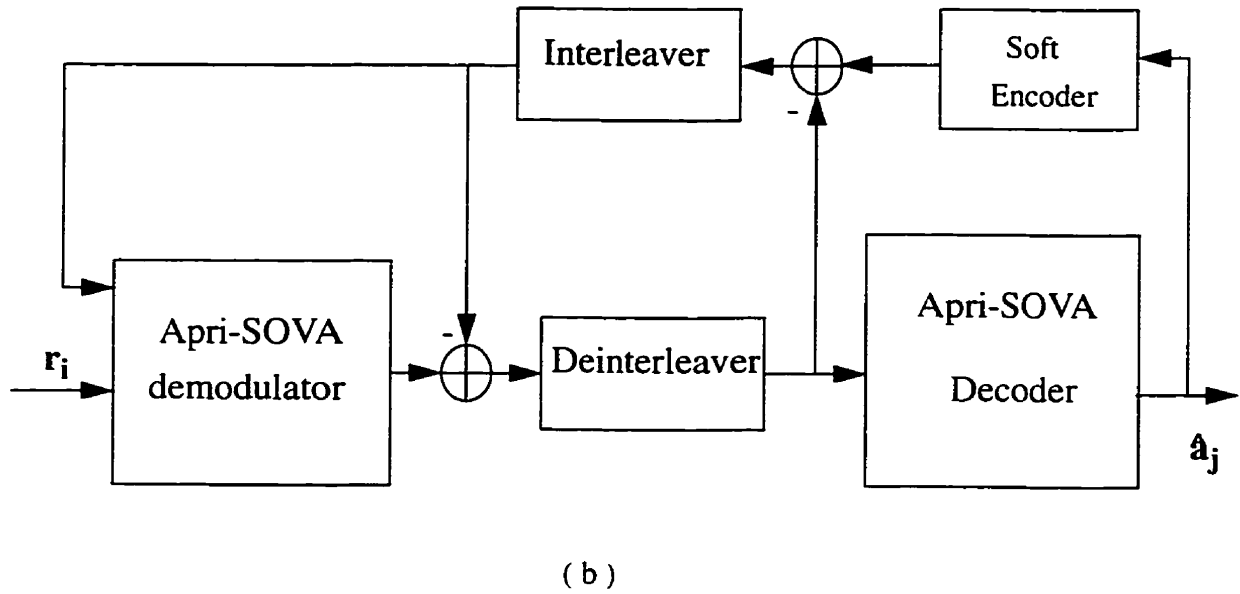


Figure 4.1 Apri-SOVA demodulator (4.1 (a)) and an iterative Apri-SOVA receiver (4.1 (b))

son and Hoehner [36-38] and applied to iteratively decode concatenated codes (e.g. turbo codes). It is not repeated here. Only the differences, namely the definition and calculation of the branch metric used in Apri-SOVA, are discussed in this section.

Apri-SOVA is a maximum likelihood sequence estimator, which searches for the possible transmitted sequence $a(\mathcal{S})$ (channel input) by maximizing the a posteriori probability:

$$\max_{\mathcal{S}} P[a(\mathcal{S}) | r_i^{\alpha N}] \quad (4.1)$$

Since

$$P[a(\mathcal{S}) | r_i^{\alpha N}] = P[r_i^{\alpha N} | a(\mathcal{S})] \cdot \frac{P(a(\mathcal{S}))}{P[r_i^{\alpha N}]} \quad (4.2)$$

then

$$\max_{\mathfrak{S}} P[a(\mathfrak{S}) | r_1^{\alpha N}] = \frac{1}{P[r_1^{\alpha N}]} \cdot \max_{\mathfrak{S}} \{P[r_1^{\alpha N} | a(\mathfrak{S})] \cdot P(a(\mathfrak{S}))\} \quad (4.3)$$

The problem has been changed to find the possible transmitted sequence $a(\mathfrak{S})$ by maximizing the probability:

$$\max_{\mathfrak{S}} \{P[r_1^{\alpha N} | a(\mathfrak{S})] \cdot P(a(\mathfrak{S}))\} \quad (4.4)$$

Let $M_k^{(s)}$ be the partial path metric of path \mathfrak{S} at time k , and define

$$M_k^{(s)} = \log \{P[r_1^{\alpha k} | a^k(\mathfrak{S})] \cdot P[a^k(\mathfrak{S})]\} \quad (4.5)$$

From Eq(3.8)

$$P[r_1^{\alpha k} | a^k(\mathfrak{S})] = \prod_{l=1}^{\alpha k} P(r_l | Y_{l-1}(\mathfrak{S})) \quad (4.6)$$

one has

$$\begin{aligned} e^{M_k^{(s)}} &= \prod_{l=1}^{\alpha k} P[r_l | Y_{l-1}(\mathfrak{S})] \cdot \prod_{l=1}^k P[a_l(\mathfrak{S})] \\ &= \prod_{l=\alpha(k-1)+1}^{\alpha k} P[r_l | Y_{l-1}(\mathfrak{S})] \cdot P[a_k(\mathfrak{S})] \cdot \prod_{l=1}^{\alpha k - \alpha} P[r_l | Y_{l-1}(\mathfrak{S})] \cdot \prod_{l=1}^{k-1} P[a_l(\mathfrak{S})] \\ &= \prod_{l=\alpha(k-1)+1}^{\alpha k} P[r_l | Y_{l-1}(\mathfrak{S})] \cdot P[a_k(\mathfrak{S})] \cdot e^{M_{k-1}^{(s)}} \end{aligned} \quad (4.7)$$

Take the logarithm of both sides to obtain:

$$M_k^{(s)} = M_{k-1}^{(s)} + \sum_{l=\alpha(k-1)+1}^{\alpha k} \log P[r_l | Y_{l-1}(\mathfrak{S})] + \log P[a_k(\mathfrak{S})] \quad (4.8)$$

Now let constant C be

$$C = \log P(a_k = 1) + \log P(a_k = 0) \quad (4.9)$$

It is well known that the maximum will not change if a constant $(-C/2)$ is added. Therefore

$$\begin{aligned} \max_{\mathcal{S}} \{M_k^{(\mathcal{S})}\} &= \max_{\mathcal{S}} \left\{ M_{k-1}^{(\mathcal{S})} + \sum_{l=\alpha(k-1)+1}^{\alpha k} \log P[r_l | Y_{l-1}(\mathcal{S})] + \log P[a_k(\mathcal{S})] \right\} \\ &= \max_{\mathcal{S}} \left\{ M_{k-1}^{(\mathcal{S})} + \sum_{l=\alpha(k-1)+1}^{\alpha k} \log P[r_l | Y_{l-1}(\mathcal{S})] + \log P[a_k(\mathcal{S})] - \frac{1}{2} \cdot C \right\} \end{aligned}$$

Consider

$$\log P[a_k(\mathcal{S})] - \frac{1}{2} \cdot C = \begin{cases} \frac{1}{2} \cdot \log \frac{P(a_k = 1)}{P(a_k = 0)} & a_k(\mathcal{S}) = 1 \\ -\frac{1}{2} \cdot \log \frac{P(a_k = 1)}{P(a_k = 0)} & a_k(\mathcal{S}) = 0 \end{cases}$$

Then

$$\begin{aligned} \max_{\mathcal{S}} \{M_k^{(\mathcal{S})}\} &= \max_{\mathcal{S}} \left\{ M_{k-1}^{(\mathcal{S})} + \sum_{l=\alpha(k-1)+1}^{\alpha k} \log P[r_l | Y_{l-1}(\mathcal{S})] + \right. \\ &\quad \left. \frac{1}{2} \cdot [2a_k(\mathcal{S}) - 1] \cdot \log \frac{P(a_k = 1)}{P(a_k = 0)} \right\} \end{aligned}$$

and the following recursion is obtained:

$$\begin{aligned} M_k^{(\mathcal{S})} &= M_{k-1}^{(\mathcal{S})} + \sum_{l=\alpha(k-1)+1}^{\alpha k} \log P[r_l | Y_{l-1}(\mathcal{S})] + \\ &\quad \frac{1}{2} \cdot [2a_k(\mathcal{S}) - 1] \cdot \log \frac{P(a_k = 1)}{P(a_k = 0)} \quad (4.10) \end{aligned}$$

The second term in above equation is the branch metric, which can be calculated with the

Kalman filter. The last term: $\frac{1}{2} \cdot [2a_k(\hat{S}) - 1] \cdot \log \frac{P(a_k = 1)}{P(a_k = 0)}$ is a priori information supplied

by the Apri-SOVA decoder when the iterative Apri-SOVA processing technique is applied.

Fig. 4.2 shows how metric $M_k^{(s)}$ works. When the channel is poor, the last term is usually larger than second term of Eq(4.10) and demodulation will depend on this soft information; otherwise the branch metric will be larger and demodulation will rely on the observation r_1^k .

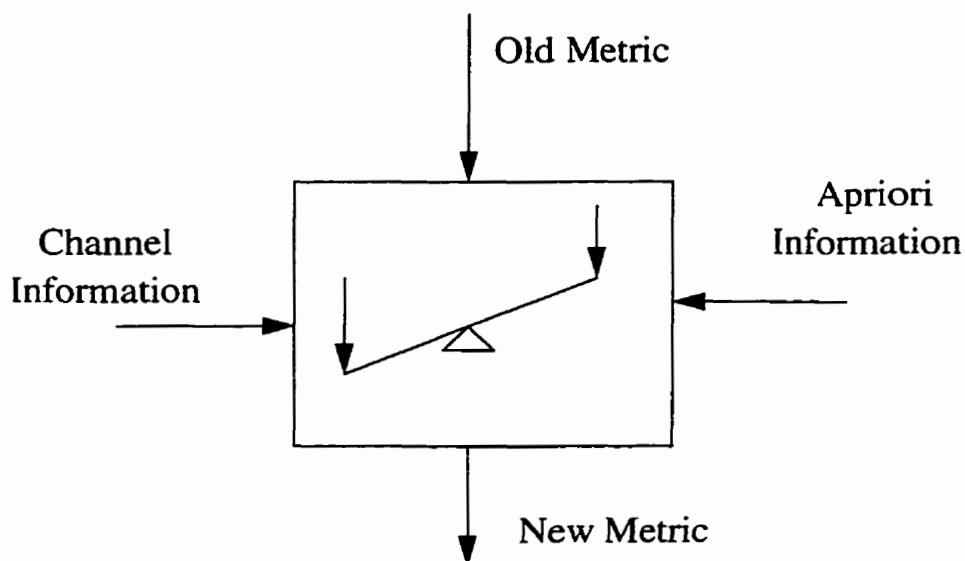


Figure 4.2 The metric for Apri-SOVA demodulation

4.2 Iterative demodulation and decoding with Apri-SOVA

Fig. 4.1(b) gives the structure of iterative Apri-SOVA demodulation and decoding, the decoder delay is not taken into account in this figure. During the first iteration, the Apri-SOVA demodulator is fed with the sufficient statistic \hat{r} , the extrinsic information $LLR(a_j)$ supplied by Apri-SOVA decoder is zero at this time. The data \hat{r} is processed by the demodulator and the soft-output is sent to the deinterleaver and the Apri-SOVA decoder. If only one iteration is required, the decision will be made based on the soft value of the SOVA decoder. When many iterations are required, these soft values will be sent to a soft-encoder to realize the symbol-to-coded-bit probability conversion. Then the soft value (extrinsic information) is generated and sent to the interleaver and finally feedback to the Apri-SOVA demodulator.

4.2.1 Convolutional code

The convolutional code used in this chapter is the (2,1,6) convolutional code. Its generator sequences are:

$$g_1(x) = (1011011) \quad g_2(x) = (1111001) \quad (4.11)$$

4.2.2 Metric for Apri-SOVA decoder

The derivation of the metric for the Apri-SOVA decoder is similar to the one for the Apri-SOVA demodulator, and is not repeated in this section. Only the recursion result is given:

$$M_k^{(\mathcal{S})} = M_{k-1}^{(\mathcal{S})} - d_k + \sum_{j=r(k-1)+1}^{rk} \frac{1}{2} \cdot (2a_j - 1) \cdot LLR(a_j) \quad (4.12)$$

where the last term is the soft-output of the Apri-SOVA demodulator, r is the coding rate of the convolutional code; the branch metric d_k is the Hamming distance.

4.2.3 Soft-encoder

The soft-value $LLR(c_n)$ of the SOVA decoder is the soft information about the symbol bit c_n , while the soft information $LLR(a_j)$ needed to feedback to the SOVA demodulator is about the coded bit a_j . Therefore it is necessary to convert the $LLR(c_n)$ into $LLR(a_j)$ before it is fed back to the demodulator.

A soft-encoder is designed based on the likelihood algorithm of a binary random variable proposed by Hagenauer [30]. Let u be a binary random variable where $u \in \{0, 1\}$. 0 is a null element under addition \oplus . As defined in chapter 3, the soft-value $L(u)$ can be written as:

$$L(u) = \log \frac{P(u=1)}{P(u=0)} \quad (4.13)$$

In likelihood algebra, the addition \boxplus is defined as [30] follows

$$L(u_1) \boxplus L(u_2) = L(u_1 \oplus u_2) \quad (4.14)$$

with the rules

$$L(u) \boxplus \infty = L(u) \quad (4.15)$$

$$L(u) \boxplus 0 = 0 \quad (4.16)$$

When u_1 and u_2 are statistically independent,

$$\begin{aligned}
L(u_1) \boxplus L(u_2) &= L(u_1 \oplus u_2) = \log \frac{P(u_1 \oplus u_2 = 1)}{P(u_1 \oplus u_2 = 0)} \\
&= \log \frac{P(u_1 = 1) \cdot P(u_2 = 0) + P(u_1 = 0) \cdot P(u_2 = 1)}{P(u_1 = 1) \cdot P(u_2 = 1) + P(u_1 = 0) \cdot P(u_2 = 0)} \\
&= \log \frac{\frac{1}{1 + e^{L(u_1)}} \cdot \frac{e^{L(u_2)}}{1 + e^{L(u_2)}} + \frac{1}{1 + e^{L(u_2)}} \cdot \frac{e^{L(u_1)}}{1 + e^{L(u_1)}}}{\frac{1}{1 + e^{L(u_1)}} \cdot \frac{1}{1 + e^{L(u_2)}} + \frac{e^{L(u_2)}}{1 + e^{L(u_2)}} \cdot \frac{e^{L(u_1)}}{1 + e^{L(u_1)}}} \\
&= \log \frac{e^{L(u_1)} + e^{L(u_2)}}{1 + e^{L(u_1)} \cdot e^{L(u_2)}} \\
&\approx -\text{sign}(L(u_1)) \cdot \text{sign}(L(u_2)) \cdot \min(|L(u_1)|, |L(u_2)|) \quad (4.17)
\end{aligned}$$

Extending the above result to J variables

$$\begin{aligned}
\sum_{\boxplus, j=1}^J L(u_j) &= L \left(\sum_{\oplus, j=1}^J u_j \right) \\
&\approx -\prod_{j=1}^J \text{sign}(L(u_j)) \cdot \min|L(u_j)| \quad (4.18)
\end{aligned}$$

Based on Eq (4.18), the following soft encoder of Fig. 4.3 is obtained.

4.3 Simulation Results

The same frequency selective Rayleigh fading channel as in Chapter 3 was studied with the Apri-SOVA algorithm. Fig. 4.4. shows a similar block diagram used by the simulation.

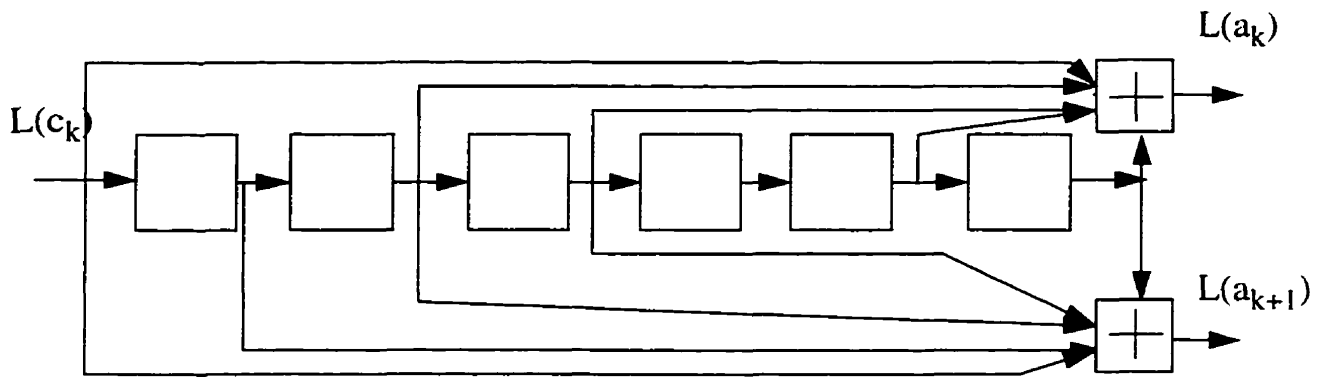


Figure 4.3 (2,1,6) Soft Encoder

The input sequence length varied with the SNR and was divided into frames of 2560 bits. The interleaver used in the simulation is a 40x64 block interleaver, and the Apri-SOVA demodulation and decoding are given in the previous section. The simulations were done on Sun stations over a SNR range of 5-20 dB, and two different fading rates, $b = 0.05$, and $b = 0.005$, are used in the simulations.

Fig. 4.5 shows the bit error probabilities (BER) of Apri-SOVA demodulation for the frequency selective Rayleigh fading channel. The convolutional encoder and interleaver are not used in this simulation. Fig. 4.6. gives the BER for Apri-SOVA demodulation and decoding with the (2,1,6) convolution code and interleaver. The error performance of the iterative Apri-SOVA receiver using a (2,1,6) convolutional code and interleaver are given in Fig. 4.7 and Fig. 4.8. Figure 4.7 is for a slower fading channel ($b = 0.005$) and the faster one ($b = 0.05$) is shown in Fig. 4.8. Up to 3 iterations have been performed. It can be seen that the most significant gain is obtained with the

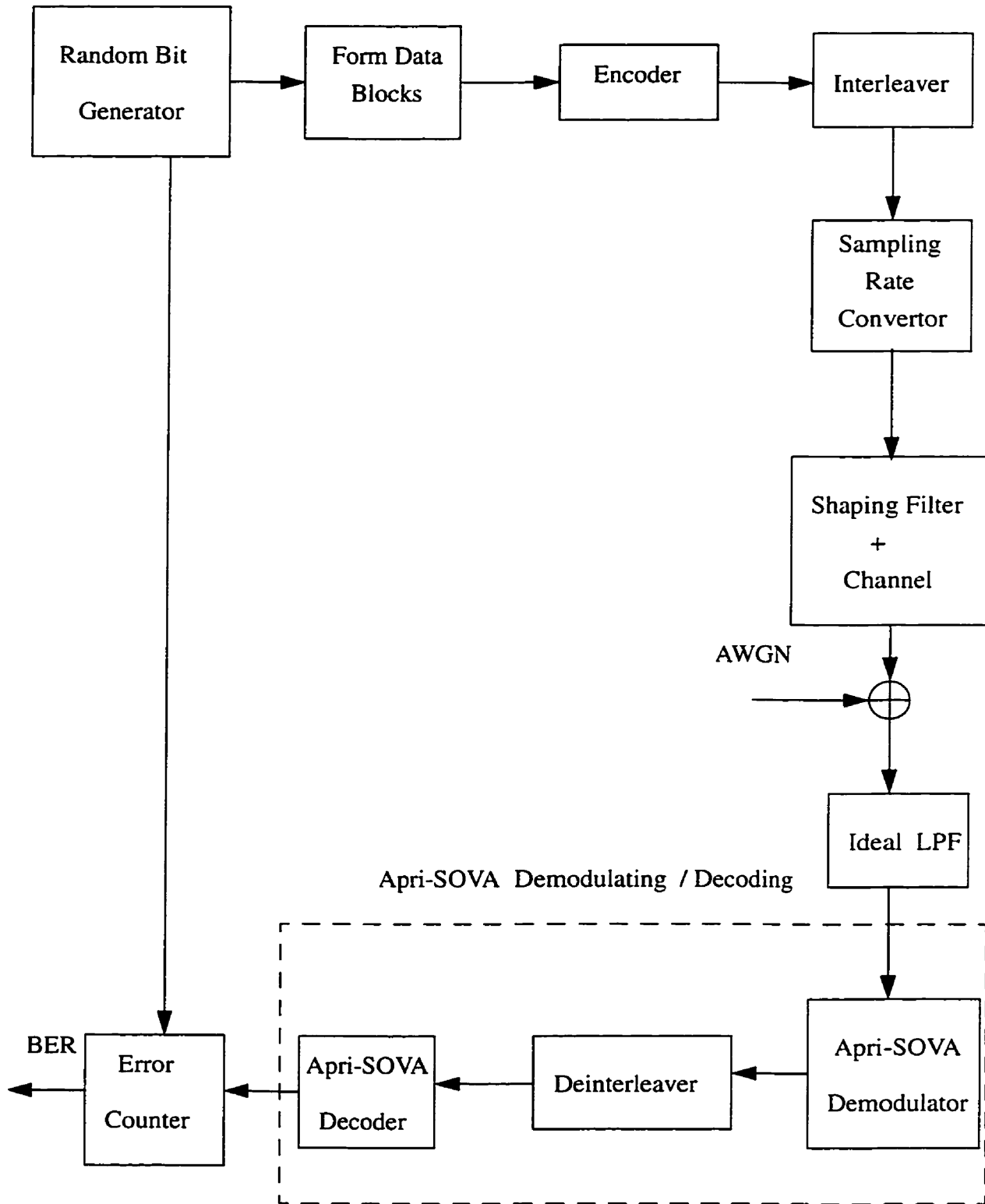


Figure 4.4 Simulation Block Diagram for the Apri-SOVA Receiver

first and second iteration. A coding gain of 2.5dB is achieved at a bit error rate level of 10^{-4} for the slowly fading channel with one iteration (Fig. 4.7). For fast fading, the BER changes from 2×10^{-3} to 2×10^{-4} at 15dB and from 3×10^{-4} to 8×10^{-5} at 20dB after one iteration (Fig. 4.8). It is of interest to compare the above results with the ones in [23], where SSE (Sequential Sequence Estimator) with the same convolutional code is used. It is found that for the slowly fading channel, the BER of the iterative Apri-SOVA is very close to the one of SSE with coding after the first iteration, and improves from 7×10^{-4} to 3×10^{-4} at 15dB after the third iteration. Since in [23] the optimal demodulation and decoding are performed in one stage, i.e. the results are optimal, this means the performance of the iterative Apri-SOVA is close to the optimal. The reason that the BER of the iterative Apri-SOVA is better than that of SSE after several iterations is that the interleaver can not be used in [23] for the reason of computational complexity. Also for the fast fading channel, the BER improves from 3×10^{-3} (SSE) to 2×10^{-4} (Apri-SOVA) at 15dB and 6×10^{-4} to 8×10^{-5} at 20dB after three iterations (Fig. 4.8). Finally the simulation results in this chapter indicate that an irreducible error floor still exists in both cases, which says that though coding, interleaving and even iteration can improve the BER, they cannot remove the error floor caused by the Rayleigh fading channel with ISI. Finally compared to the results of Chapter 3, the simulation results in this Chapter indicates that a better error performance can be obtained with large size interleaver and channel encoder, which indicates that the Apri-SOVA receiver is more attractive.

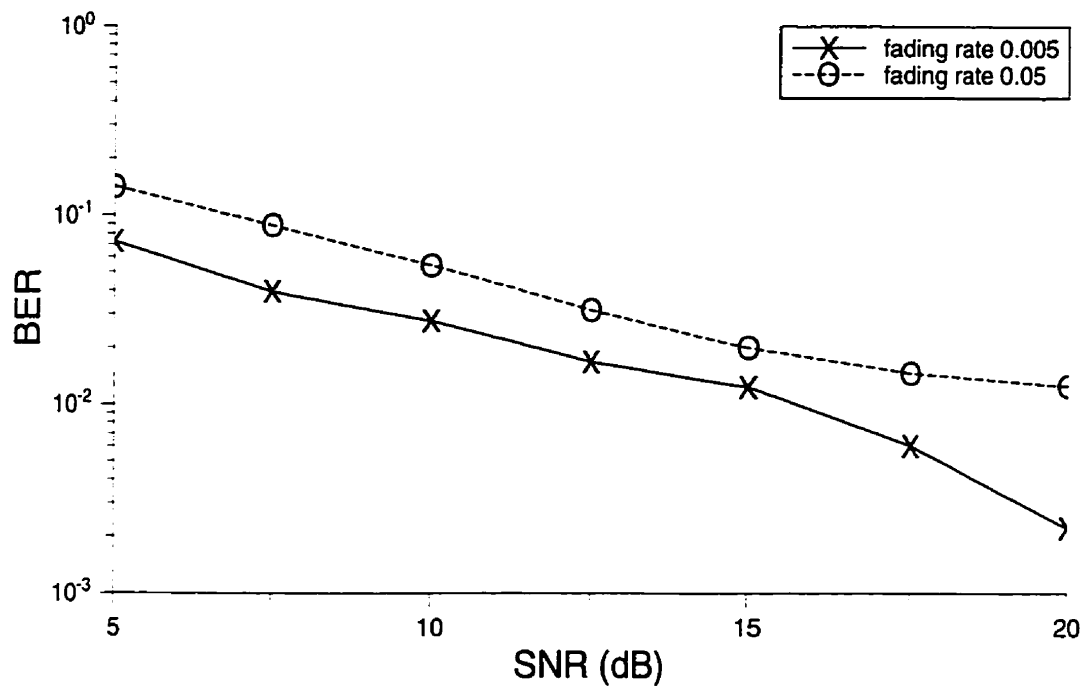


Figure 4.5 BER performance of Apri-SOVA demodulation for frequency selective Rayleigh fading channel

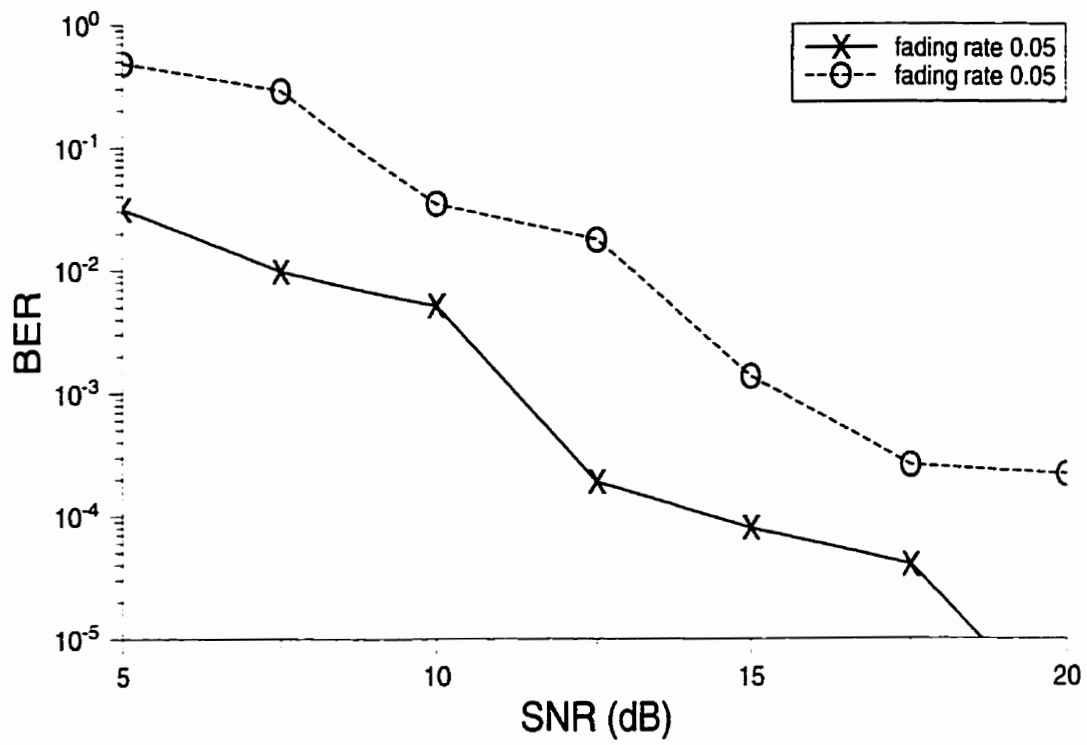


Figure 4.6 BER performance of Apri-SOVA demodulating and decoding for frequency selective Rayleigh fading channel

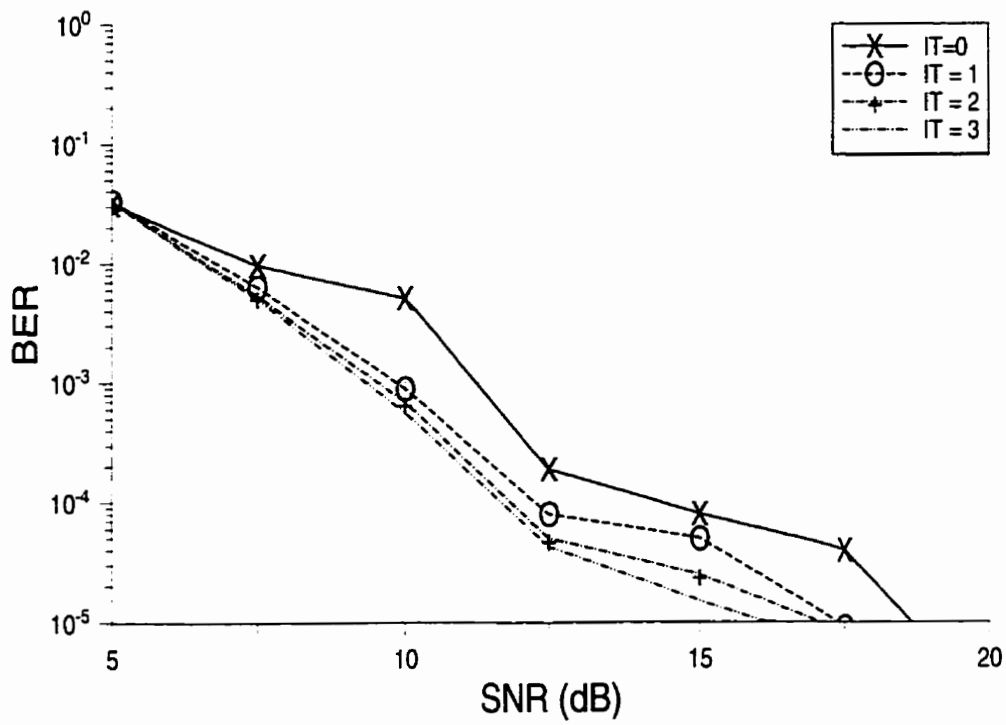


Figure 4.7 BER performance of iterative Apri-SOVA receiver for slow fading channel

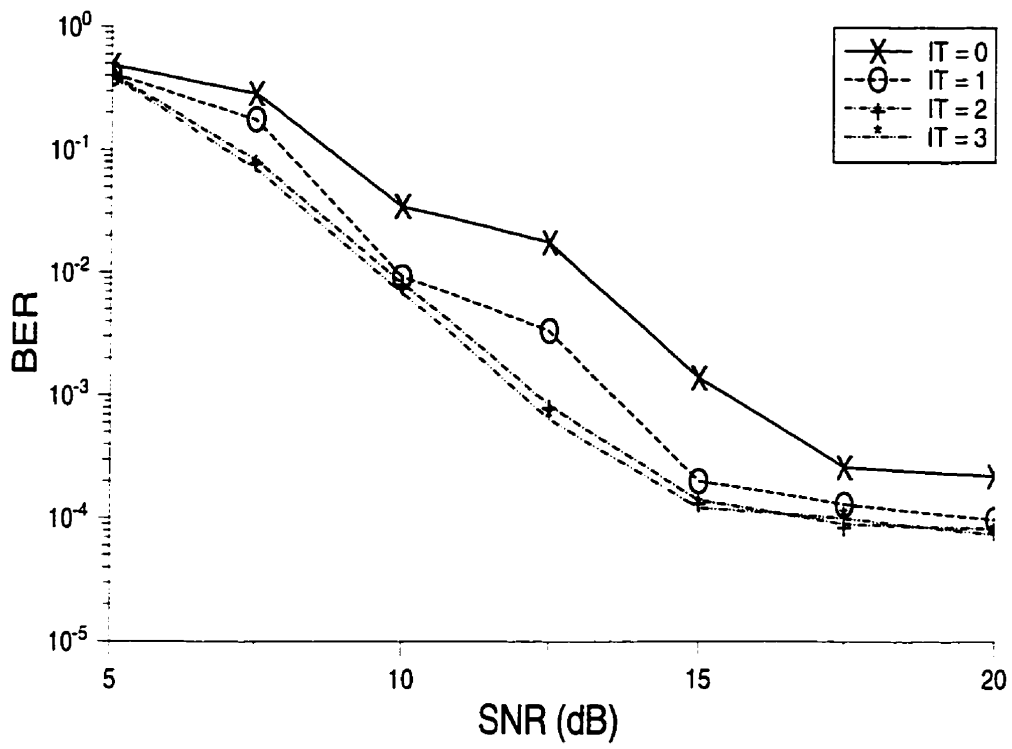


Figure 4.8 BER performance of iterative Apri-SOVA receiver for fast fading channel

Chapter 5

Conclusions

5.1 Conclusions

The transmitter of a modern communication system is usually composed of channel encoders, interleavers, and a modulator. All of these units contain memory which makes optimal demodulation and decoding in one stage impractical. One possible solution is to perform the demodulation and decoding into several stages, but as discussed in chapter 1, its performance can be far from optimal.

In this thesis, an iterative MAP receiver and an iterative Apri-SOVA receiver have been developed for joint demodulation and decoding of signals transmitted over the frequency selective Rayleigh fading channel. The work of [16,21] is extended. The symbol-by-symbol MAP algorithm for demodulating of the signal over the frequency selective Rayleigh fading channel is first derived and based on it, a two stage suboptimal iterative MAP receiver is proposed. The error performance of the receiver in the frequency selective Rayleigh fading channel has been studied with computer simulation. The results indicate that a coding gain of 3dB can be achieved at a bit error rate level of 10^{-3} for the slowly fading channel with the first iteration. For the fast one, the BER changes from 10^{-2} to 6×10^{-3} at 10dB and from 3×10^{-2} to 8×10^{-3} at 15dB after one iteration.

As is well known that the MAP algorithm is complex with respect to computation, especially

when the size of interleaver is larger than 400. The results for the turbo code indicate that the large interleaver (size > 1000) usually improves the BER performance. Therefore it is useful to study a simple soft-in, soft-out algorithm which can be applied with a large interleaver size. An iterative Apri-SOVA receiver is developed to replace the iterative MAP receiver in chapter 4. After deriving the required metric to be used in the Apri-SOVA demodulator and decoder, a two stage Apri-SOVA receiver was proposed and iteration is also carried out with the help of a soft encoder. Since in Apri-SOVA a sliding-window method is used, a large size interleaver can be used without increasing the computation complexity. The computer simulation is done on the same frequency selective Rayleigh fading channel as in chapter 3 to study the error performance of the proposed iterative receiver. A coding gain of 2.5dB is achieved at a bit error rate level of 10^{-4} for a slowly fading channel with the first iteration. For fast fading, the BER changes from 2×10^{-3} to 2×10^{-4} at 15dB and from 3×10^{-4} to 8×10^{-5} at 20dB after the first iteration. Comparing the above results with the ones in [23], where SSE with the same convolutional code is used, it is found that for the slowly fading channel, the BER of the iterative Apri-SOVA with the first iteration is very close to the one of SSE with coding, and it improves from 7×10^{-4} to 3×10^{-4} at 15dB after three iterations. In [23], the optimal demodulation and decoding are performed in one stage so the results are optimal, which means the performance of the iterative Apri-SOVA is close to the optimal. The reason that the BER of the iterative Apri-SOVA is better than that of the SSE after several iterations is that the interleaver can not be used in [23] for the reason of computational complexity. Also for the fast fading channel, the BER improves from 3×10^{-3} (SSE) to 2×10^{-4} (Apri-SOVA) at 15dB and 6×10^{-4} to 8×10^{-5} at 20dB after three iterations. Finally, compared to the results of chapter 3, the simulation results in chapter 4 indicate that a better error performance can be obtained with a large size interleaver and channel encoder, which says that the Apri-SOVA

receiver is more attractive.

5.2 Suggestions for further study

Some questions remain unanswered and they may be of interest for further study.

1) Some efficient modulation schemes, like PSK, CPM and TCM, are not studied in this thesis. With the help of pilot-aided channel estimation methods, MAP and Apri-SOVA joint demodulation and decoding of the above signals is possible.

2) The Kalman filter is used to estimate the channel impulse response in this thesis, but it does not use the soft information supplied by the soft decoder in its channel estimation. Studying a channel estimator which can use some a priori information may be an interesting topic. In that case, a better channel estimation can be obtained and iterative demodulation and decoding should give a better BER performance.

3) The “uniform interleaver” is an interesting concept [39-40]. It can be used to study the average BER performance of iterative MAP and Apri-SOVA receivers.

References:

- [1] K. Brayer, "Error control Techniques Using Binary Symbol Burst Codes". IEEE Trans. on Commun., Vol. 16, No. 2, pp.199-214, April 1968
- [2] D. G. Brennan, "Linear Diversity Combining Techniques", Pro. IRE., Vol. 47, pp. 1075-1102, June, 1959
- [3] J. N. Pierce and S. Stein, "Multiple Diversity with Nonindependent Fading". Proc. of IRE, Vol. 48, Jan. 1960
- [4] G C. Porter, "Error Distribution and Diversity performance of a Frequency-Differential PSK HF modem", IEEE Trans. on. Commun., Vol., 16, Aug. 1968
- [5] S. U. H. Qureshi, "Adaptive Equalization", IEEE Proceedings, Vol. 73, No. 9, pp. 1349-1387, Sept. 1985
- [6] M. E. Austin, "Decision-Feedback Equalization for Digital Communication Over Dispersive Channel", M.I.T. Research Lab. on Electr. Tech. Report 461, Aug. 1967
- [7] E. Eleftheriou, and D. Falconer, "Adaptive Equalization Techniques for HF Channels", IEEE Journal on Selected Area in Communications, Vol.5, No.2, pp.238-247, Feb. 1987
- [8] R. A. Ziegler and J. M. Cioffi, "Estimation of Time-Varying Digital Radio Channel", IEEE Trans. on Vehicular Tech., Vol 41, No.2, pp134-151, May 1992
- [9] G. D. Forney, Jr, "Maximum Likelihood Sequence Estimation of Digital Sequence in the Pres-ence of Intersymbol Interference" IEEE Trans on Information Theory, Vol. IT-18, pp363-378, May 1972
- [10] F. R. Magee, Jr. and J. G. Proakis, "Adaptive Maximum Likelihood Sequence Estimation for Digital Signalling in the Presence of Intersymbol Interference", IEEE Trans on Information Theory, Vol. IT-19, pp.120-124, Jan. 1973

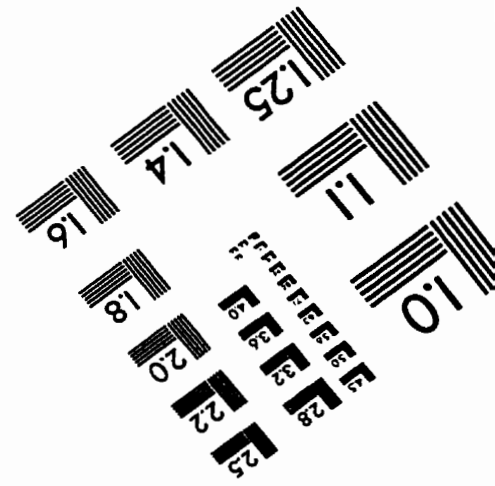
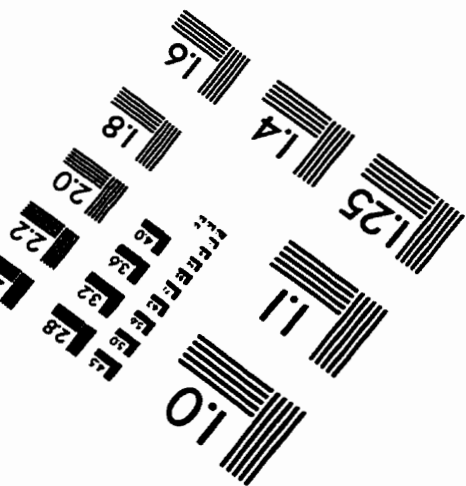
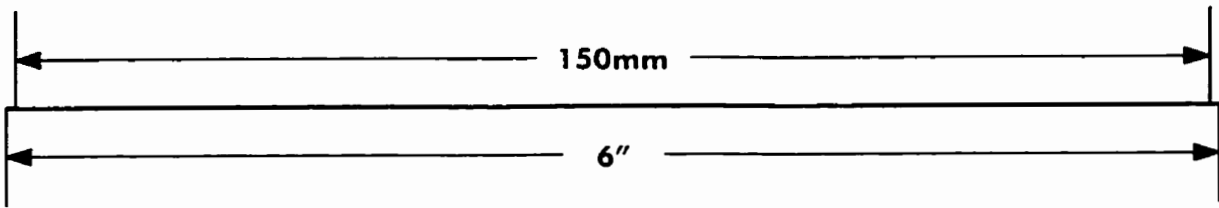
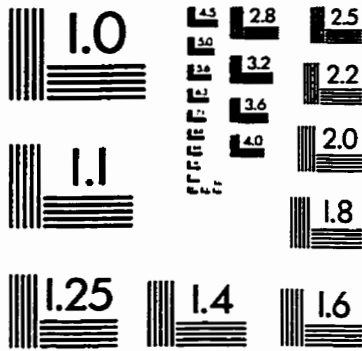
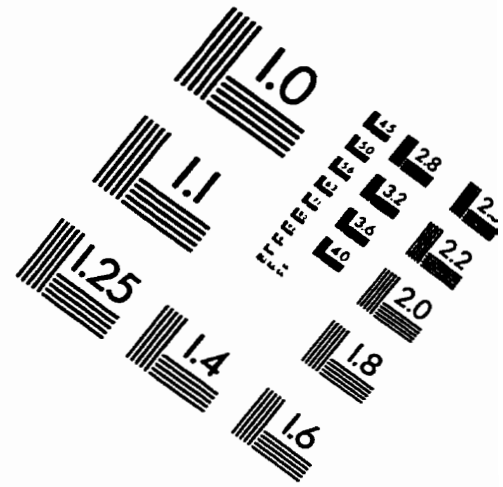
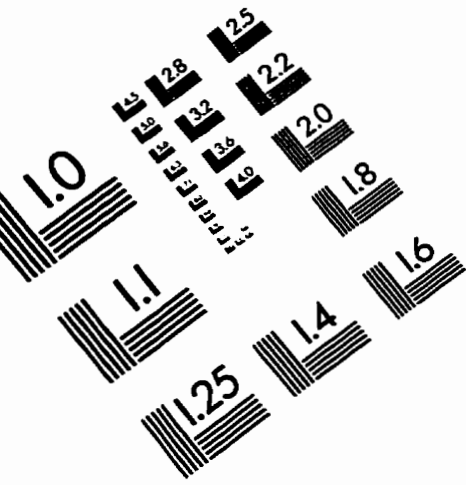
- [11] G. Ungerboeck, "Adaptive Maximum Likelihood Receiver for Carrier Modulated Data Transmission System", IEEE Trans. on Commun., Vol. 22, May 1974
- [12] S. Crozier, D. Falconer, and S. Mahmond, "Short-Block Equalization Techniques Employing Channel Estimation for Time-Dispersive Channels", 39th IEEE VTC, Vol.I, pp. 142-146, May, 1989
- [13] A. N. D'Andrea, A. Diglio and U. Mengali, "Symbol-Aided Channel Estimation with Nonselective Rayleigh Fading Channel", IEEE Trans. on. Vehicular Tech. Vol. 44, No.1, pp.41-48, 1995
- [14] H. Kong, Receiver Structure for Wireless Mobile Channels, Ph.D. Thesis, University of Manitoba, 1997
- [15] J. H. Lodge and M. L. Moher, "Maximum Likelihood Sequence Estimation of CPM signals Transmitted Over Rayleigh Flat-Fading Channels", IEEE Trans. on Commun., Vol.38, No.6, pp.787-794, Jun. 1990
- [16] Q. Dai and E. Shwedyk, "Detection of Bandlimited Signals Over Frequency Selective Fading Channels", IEEE Trans. on Commun., Vol.42, No. 3, pp.941-950, March 1994
- [17] X. Yu, and S. Pasupathy, "Innovations-Based MLSE for Rayleigh Fading Channels", IEEE Trans. on Commun., Vol. 43, No.2/3/4, pp1534-1544, Feb./Mar./Apr., 1995
- [18] M. E. Rollins and S. J. Simmons, "Reduced-Search Blind Trellis Decoders for Frequency-Selective Rayleigh Fading Channels", Proc. of IEEE Pacific Rim Conf. on Commun., Computer & Signal Processing, pp.305-309, Victoria,BC, Canada, May, 1993
- [19] C. Berrou, A. Glavieux and P. Thitimajshima, "Near Shannon Limit Error-Correcting Coding and Decoding: Turbo-Codes(1)", Proc. ICC'93, pp.1064-1070, May, 1993
- [20] P. Roberston, "Illuminating the Structure of Decoders for Parallel Concatenated Recursive

- Systematic (Turbo) Codes”, Proc. IEEE GLOBECOM’94, San Francisco, CA, pp.1298-1303, Dec. 1994
- [21] M. J. Gertsman and J. H. Lodge, “Symbol-by-Symbol MAP Demodulation of CPM and PSK signals on Rayleigh Flat-Fading Channels”, IEEE Trans. on Commun. Vol.45, No.7, pp.788-799, July,1997
- [22] J. G. Proakis, Digital Communications, McGraw-Hill, New York, 2nd edition, 1989
- [23] Q. Dai, Sequence Estimation for Rayleigh Fading Channels with Intersymbol Interference, Ph.D. Thesis, University of Manitoba, 1993
- [24] G. L. Stuber, Principles of Mobile Communication, Kluwer Academic Publishers, 1996
- [25] M. J. Omid, S. Pasupathy, and P. G. Gulak, “Joint Data and Kalman Estimation of Fading Channel Using A Generalized Viterbi Algorithm”, preprint
- [26] B. D. O. Anderson and J. B. Moor, “Optimal Filtering”, Prentice-Hall, Endlewood Cliffs, New Jersey, 1979
- [27] H. Kong and E. Shwedyk, “Iterative Channel Estimation and Sequence Detection for Block and Convolutional Codes Over Frequency Selective RAyleigh Fading Channels”, ISITA’96, Vol. 1, pp.401-404, Victoria, Canada, Sept., 1996
- [28] L. Bahl, J. Cocke, F. Jelinek, and J. Raviv, “Optimal Decoding of Linear Codes for Minimizing Symbol Error rate”, IEEE Trans. on Inform. Theory, Vol. IT-20, pp.284-287, Mar. 1974
- [29] J. lodge, R. Young, P. Hoeher, and J. Hagenauer, “Separable MAP “Filters” for the Decoding of Product and Concatenated Codes”. Proc. IEEE Int. Conf. on Comm., pp.1740-1745, Geneva, Switzerland, May 1993
- [30] J. Hagenauer, “Source-Controlled Channel Decoding”, IEEE Trans. on. Comm., Vol.43,

No.9, pp.2449-2456, Sept. 1995

- [31] P. Jung, "Comparison of Turbo-Code Decoders Applied to Short Frame Transmission Systems", *IEEE J. Select. Areas Commun.*, Vol. 14, No. 3, pp. 530-537, April, 1996
- [32] S. Benedetto and G. Montorsi, "Iterative Decoding of Serially Concatenated Convolutional Codes", *Electron. Lett.*, Vol.32, No.13, pp.117-118, June 1996
- [33] S. Benedetto and G. Montorsi, "Serial Concatenated of Block and Convolutional Codes", *Electron. Lett.*, Vol.32, No.10 pp.887-888, May, 1996
- [34] P. Robertson, E. Villebrun, and P. Hoeher, "A Comparison of Optimal and Sub-optimal MAP Decoding Algorithm Operating in the Log Domain", *Proc. ICC'95*, pp.1009-1013, Seattle, Washington, June 1995
- [35] J. Hagenauer and P. Hoeher, "A Viterbi Algorithm with Soft-Decision Output and its Applications", *Proc. GLOBEMCOM'89*, pp.1680-1686, Nov., 1989
- [36] J. Hagenauer, P. Robertson, and L. Papke, "Iterative ("Turbo") Decoding of Systematic Convolutional Codes with the MAP and SOVA Algorithms", *Proc. ITG Cong. Vol.130*, pp.21-29, Munich, Oct., 1994
- [37] J. Hagenauer, E. Offer, and L. Papke, "Iterative Decoding of Binary Block and Convolutional Codes", *IEEE Trans. on Inform. Theory*, Vol. IT-42, No.2, pp.429-445, Mar. 1996
- [38] J. Hagenauer, P. Hoeher and J. Huber, "Soft-Output Viterbi and Symbol-by-Symbol MAP Decoding Algorithms and Applications",
- [39] S. Benedetto and G. Montorsi, "Performance of Turbo Codes", *Electron. Lett.*, Vol.31, No.3, pp.163-165, Feb. 1996
- [40] S. Benedetto and G. Montorsi, "Design of Parallel Concatenated Convolutional Codes", *IEEE. Trans. on. Commun.*, Vol.44, No.5, pp.591-600, May, 1996

IMAGE EVALUATION TEST TARGET (QA-3)



APPLIED IMAGE, Inc
1653 East Main Street
Rochester, NY 14609 USA
Phone: 716/482-0300
Fax: 716/288-5989

© 1993, Applied Image, Inc., All Rights Reserved